ARTICLE | OPEN ACCESS

Drug Discovery

To Cite:
Alawode T, Lajide L. An Investigation of *Crinum jagus* Bulbs for Lead Anti-Hepatocellular Carcinoma Compounds. *Drug Discovery* 2024; 18: e19dd2003
doi: https://doi.org/10.54905/dissi.v18i42.e19dd2003

Author Affiliation:
[1]Department of Chemistry, Federal University Otuoke, Nigeria
[2]Department of Chemistry, Federal University of Technology Akure, Nigeria

[*]**Corresponding Author**
Department of Chemistry, Federal University Otuoke, Nigeria
Email: onatop2003@yahoo.com

Peer-Review History
Received: 09 July 2024
Reviewed & Revised: 13/July/2024 to 10/October/2024
Accepted: 15 October 2024
Published: 19 October 2024

Peer-Review Model
External peer-review was done through double-blind method.

Drug Discovery
pISSN 2278–540X; eISSN 2278–5396

DISCOVERY SCIENTIFIC SOCIETY

An Investigation of *Crinum jagus* Bulbs for Lead Anti-Hepatocellular Carcinoma Compounds

Taye Alawode[1*], Labunmi Lajide[2]

ABSTRACT

Hepatocellular carcinoma is one of the primary causes of cancer-related mortality. In this study, we evaluated the anticancer activity of five chromatographic fractions derived from the methanol extract of *Crinum jagus* bulbs against the HepG2 hepatocellular carcinoma cell line, using the MTT (3-(4,5-dimethylthiazol-2-yl)-2,5-diphenyltetrazolium bromide) assay. The IC50 value was used as a measure of anticancer activity. The most active fraction was analyzed using GCMS and LCMS. The binding energies of the identified compounds with Caspase-3, Caspase-9, and EGFR were evaluated and compared to those of the standard drug, Sorafenib. The compounds' drug-likeness was assessed by applying Lipinski's rule of five. The most potent fraction exhibited an IC50 value of 37 µg/ml. Nineteen (19) compounds, primarily fatty acids, fatty acid esters, and flavonoids, were identified from the fraction by GCMS and LCMS analysis. Of the nineteen (19) compounds identified in the most active fraction, linoelaidic acid (-8.23 kcal mol-1), hexadecanoic acid (-7.96 kcal mol-1) and 9,12-Octadecadienoic acid (-7.78 kcal mol-1) had a better binding affinity for Caspase-3 than Sorafenib; hexadecanoic acid methyl ester (-8.10 kcal mol-1) and pentyl linoleate (-8.00 kcal mol-1) had comparable binding energy with Sorafenib (-8.47 kcal mol-1) against Caspase-9. In contrast, hexadecanoic acid (-8.29 kcal mol-1), linoelaidic acid (-8.58 kcal mol-1), and pentyl linoleate (-8.66 kcal mol-1) had better binding energy than Sorafenib (-8.24 kcal mol-1) against EGFR. These compounds passed Lipinski's test for drug-likeness. The study's findings lend credence to the plant's traditional use as a cancer remedy.

Keywords: *Crinum jagus*, LCMS, GCMS, HepG2, molecular docking

1. INTRODUCTION

Globally, hepatocellular carcinoma (HCC) is the fourth most frequent cause of cancer-related death. The disease has a low survival rate and is widespread in sub-Saharan Africa, where factors such as aflatoxin exposure, hepatitis B and C infections, cigarette smoking, and alcohol consumption play a role in its spread (Mak and

Kramvis, 2021). Hepatocellular carcinoma is treated using chemotherapy and radiotherapy; however, these therapeutic options have not improved the survival rate among liver cancer patients significantly (Mustafa et al., 2023). Furthermore, the disease continues to be associated with high mortality because of inadequate diagnostic biomarkers and therapeutic strategies (Parikh et al., 2023). There is still a pressing need to find more affordable, more potent, and less toxic drugs.

In Nigeria, traditional medicines hold significant importance in the healthcare system. A contributing factor to the prevalence of herbal medicine among the Nigerian populace is the availability of vast and diverse vegetation. From indigenous knowledge of the medicinal uses of plants available in different parts of the world, scientists have isolated several compounds of great pharmacological importance from plants. Such compounds include the well-known anticancer drugs Vincristine and Vinblastine. Plants remain a vital source of lead compounds for fueling the drug discovery pipeline, especially because only a fraction of the world's flora and fauna have been explored for bioactivity (Howes et al., 2020).

In southwestern Nigeria, traditional healers use the bulb of *Crinum jagus* to treat cancer. *Crinum jagus* belongs to the family *Amaryllidacae*. Many extracts, as well as compounds isolated from *Crinum* species, possess potent cytotoxic and anticancer activities. For example, 6-hydroxycrinamine showed activity against BL-6 mouse melanoma cells Nair et al., (1998); criasbetaine was active against P-388 and KB *in vitro* Ghosal et al., (1986); and *C. asiaticum* leaves extracts were cytotoxic against murine P388 D1 cells (Ahmad, 1996). Previous studies show that *Crinum jagus* bulbs possess cytotoxic Salawu et al., (2020), hypoglycemic Mohammed et al., (2014), antimycobacterial, and antiplasmodial Akintola et al., (2013) properties. Previous studies reported the presence of several alkaloids in *Crinum jagus* bulbs (Ka et al., 2020; Kouadio et al., 2020).

Researchers have developed several chemical and biological screening methods to accelerate the drug discovery process. While the biological screening process utilizes various biological assays to select promising extracts or fractions for further studies Osakwe, (2016), the chemical screening approach employs several hyphenated techniques to characterize the extract in real time. According to Patel et al., (2010), the chemical screening technique provides some initial insight into the phytoconstituents of the extract and, consequently, its potential medicinal benefits. Although various hyphenated methods exist, High-Performance Liquid Chromatography-Mass Spectrometry (HPLC-MS or HPLC-MS/MS) is particularly well-suited for natural products research, as it can be used to analyze non-volatile plant constituents (Kumar, 2017).

The GC–MS technique also possesses unique advantages, including excellent chromatographic separation power, dependable quantification methods, and highly accurate metabolite identification. Unlike the LCMS technique, GC separates low molecular weight metabolites that are either volatile or, through chemical derivatization, can become volatile and thermally stable molecules. Researchers are now deploying computational tools to predict the pharmacological properties of potential drug candidates, reducing the time and huge cost associated with drug discovery (Sadybekov and Katritch, 2023). Many potential protein receptor targets involved in HCC pathogenesis, including transcription factors, growth factor receptors, apoptotic proteins, mitogen-activated protein kinases, cell division protein kinase, and serine/threonine protein kinases have been identified (Mustafa et al., 2023).

Molecular docking is employed to predict the binding orientations of ligands (from synthetic or natural sources) within the active sites of target proteins. Potential lead compounds identified through molecular docking possess a higher chance of progressing to the next level in the drug discovery process. Previously, we reported on the anticancer activity of *Crinum jagus* (J. Thomp.) Dandy leaves' extracts against the hepatocellular carcinoma (HepG2) cell line (Alawode et al., 2023). In this study, we investigate *Crinum jagus* (J. Thomp.) Dandy bulb extracts using *in vitro, in silico*, GCMS, and LCMS methods to identify potential anti-hepatocarcinoma compounds.

2. METHODS

Sample Extraction

Crinum jagus (J. Thomp.) Dandy bulbs were collected in November 2016 from the Botanical Gardens at the University of Ibadan, Nigeria. The samples were identified by Mr Kayode Owolabi, a taxonomist working with the Garden. Samples (with voucher number UIH-22441) were subsequently deposited at the University Herbarium. A total of 70 mature bulbs (with no physical damage) were transported to the laboratory in sealed containers within 24 hours of collection. In the laboratory, the bulbs were washed with distilled water and air-dried in a well-ventilated area for 21 days, and their weights were recorded. The dried bulbs were then cut into tiny pieces to ensure a uniform surface area for efficient extraction.

A 1kg dried sample was macerated in 2.5 litres of hexane for 72 hours at room temperature. The mixture was then filtered using Whatman filter paper No. 1. This process was repeated with ethyl acetate and methanol following the same procedure. The filtrates from each solvent extraction were concentrated using a rotary evaporator under reduced pressure at 40oC to yield the respective crude extracts (hexane, ethyl acetate, and methanol). The remaining dried and ground material was stored at room temperature in airtight containers for further studies. The percentage yields of the extracts were calculated using the following equation:

$$\text{Yield (\%)} = \frac{\text{Weight of Extract}}{\text{Weight of Dried Sample}} \text{ x } 100$$

Fractionation of Methanol Extract Using Column Chromatography

The methanol extract with the best yield (among the three crude extracts obtained in the previous step) was loaded on a glass column and fractionated. Briefly, twenty (20) g of the crude methanol extract was pre-adsorbed on silica gel and loaded on a glass column. The extract was eluted from the column using solvent mixtures of increasing polarity, starting with hexane, then ethyl acetate, and then methanol. A total of 115 fractions, (200 ml each) were collected from the column. Thin-layer chromatography was used to monitor these fractions, and those with similar compositions were pooled together. The five fractions obtained from this process were labelled A, B, C, D, and E. Since this study aims to identify potential anticancer compounds from the bulb of the plant, these fractions (A-E) were screened for their activity against the HepG2 cell line to determine which of them possesses the highest anticancer potential.

Anticancer screening of Fractions Against HepG2 cell line

The HepG2 cell line was obtained from the American Type Culture Collection (ATCC) (USA). Cells were grown in Dulbecco's Modified Eagle's Medium (DMEM) with 10% fetal bovine serum (FBS) and 1% penicillin-streptomycin, incubated at 37 °C in a humidified atmosphere with 5% CO2. A cell culture concentration of 2×10^3 cells/mL was prepared and plated (100 µL per well) in 96-well plates. Various concentrations (1000 µg/mL, 500 µg/mL, 250 µg/mL, 125 µg/mL, 62.5 µg/mL, 20 µg/mL, and 1 µg/mL) of the extracts, diluted in FBS-free medium, along with the standard (cisplatin), were added to each well. After 72 hours, MTT solution was added, and the cells were incubated for 3 hours. Dimethyl sulfoxide (DMSO) (100 µL) was used to dissolve the resulting purple formazan crystals. The optical density of the plant extract was then measured at 570 nm using a microplate reader (Tecan, Switzerland). Absorbance values were taken as means of triplicate measurements. The percentage of cell viability was calculated using the formula:

$$\text{Cell viability} = \frac{\text{Absorbance of Sample (mean)}}{\text{Absorbance of Control (mean)}} \text{ x } 100$$

The viability percentages were plotted against the different extract concentrations, and cytotoxicity was expressed as the IC50 value (the concentration of the compound causing 50% inhibition of cell growth). The IC50 values were obtained from the plot of percentage cell viability against fraction concentrations (Nawaz et al., 2021). Fraction B which had the best IC50 value was subjected to GCMS and LCMS Analysis to identify the compounds that are responsible for the high activity the fraction displayed against the HepG2 cell line.

GC-MS Analysis of Fraction B

Fraction B was subjected to GC-MS analysis using an Agilent 7890 gas chromatograph linked to an Agilent 5975C mass selective detector, functioning in electron impact mode. The sample components were separated using a 30 m × 0.32 mm Chrompack CP-Wax 52 CB capillary column with a 0.25 µm film thickness. The GC-MS analysis was performed under the following conditions: a diluted sample (1.0 µL) was injected at 250˚C, with helium as the carrier gas at a flow rate of 5 mL/min and an inlet pressure of 12.936 psi. The temperature of the column oven was steadily raised from 50˚C to 240˚C at a rate of 8˚C/min. The mass spectra fragmentation patterns were compared to the National Institute of Standards and Technology (NIST) Mass Spectra Library in the GC-MS database (NIST 14L) to identify the sample's constituents. A similarity index of 90 was established as the cut-off threshold for acceptance to minimize the risk of false identification.

Liquid Chromatography-Mass Spectrometry (LC-MS) Analysis of Fraction B

The LC-MS analysis of Fraction B was performed using an Agilent Hewlett-Packard 1100 chromatograph (Santa Clara, CA) fitted with an Electrospray Ionization (ESI) interface. The fraction was injected into the C-18 column (4.6 × 25 cm, 5 µm). The two components (A and B) used for linear binary gradient solvent systems are 90% acetic acid–water (A) and 10% MeOH (B). The composition of the mobile

phase was altered as follows: 10% B for 5 minutes, 10%–100% B for 20 minutes, and 100% B for 6 minutes. The flow rate was 200 μL/min. Spectra were recorded using both positive and negative ionization modes. The compounds in the extract were identified by interpreting their MS spectra and comparing them with entries in The Human Metabolome Database and the European MassBank database.

In-Silico Studies on Identified Compounds

Molecular Docking of Phytoconstituents with Proteins

SDF format files for the structures of the ligands and the standard drug (Sorafenib) were obtained from PubChem and converted into the mol2 format using the Open Babel software (O'Boyle et al., 2011). The proteins Caspase-3 (1NMS), Epidermal Growth Receptor Factor (4LQM) and Caspase-9 (2AR9) were obtained from the protein databank. The Swiss Dock server (http://www.swiss dock. ch/) was used for molecular docking (Grosdidier et al., 2011). The ligands and the proteins were uploaded onto the server. After docking, the interactions between the ligands and the proteins were visualized using the UCSF Chimera software. Models with the lowest energy indicate the most favourable interactions.

Prediction of drug-likeness of Identified Phytoconstituents

The SwissADME online web server (https://www.swissadme.ch) was used to evaluate the compounds for drug-likeness. The cutoff for drug-likeness was determined based on Lipinski's Rule of Five (Daina et al., 2017).

3. RESULTS

Percentage Yield of Extracts

Table 1 displays the percentage yields of the extracts. The methanol extract (CJBME) had the highest yield (24.68 %), while the hexane (CJBHE) and ethyl acetate (CJBEE) extracts had yields of 0.28 % and 0.44 %, respectively.

Table 1 Percentage yield of Extracts

EXTRACT	Yield (%)
CJBHE	0.28
CJBEE	0.44
CJBME	24.68

In vitro Anticancer Screening of Fractions against HepG2 cell line

Since the hexane and ethyl acetate fractions were obtained in meagre yields, they were discontinued from further studies. The methanol fraction (obtained in high yield) was loaded on a glass column and fractionated. Five fractions, labelled A, B, C, D, and E, were obtained. Figure 1 depicts the correlation between the percentage of viable HepG2 cells and the various concentrations of the fractions after 72 hours. From the graph, the IC50 values determined for fractions A, B, C, D, E, and Cisplatin are 180 μg/ml, 37 μg/ml, 250 μg/ml, 340 μg/ml, 280 μg/ml, and 5 μg/ml, respectively. Compared to the standard drug, Cisplatin (IC50 = 5 μg/ml), fraction B (IC50 = 37 μg/ml) was most effective against the HepG2 cell line.

Compounds Identified in Fraction B by GCMS Analysis

Ten (10) compounds, including fatty acids and fatty acid esters, were putatively identified from the GC-MS chromatogram of Fraction B (Figure 2). The compounds are listed in Table 2, and their structures are presented in (Figure 3). The compounds areHexadecanoic acid methyl ester (1), Hexadecanoic acid (2), Hexadecanoic acid ethyl ester (3), 9,12-Octadecadienoic acid methyl ester (4),7,10,13-Hexadecatrienoic acid, methyl ester (5), 9,12-Octadecadienoic acid (6), Linoleic acid ethyl ester (7), Linoelaidic acid (8), Pentyllinoleate (9) and Stigmasterol (10).

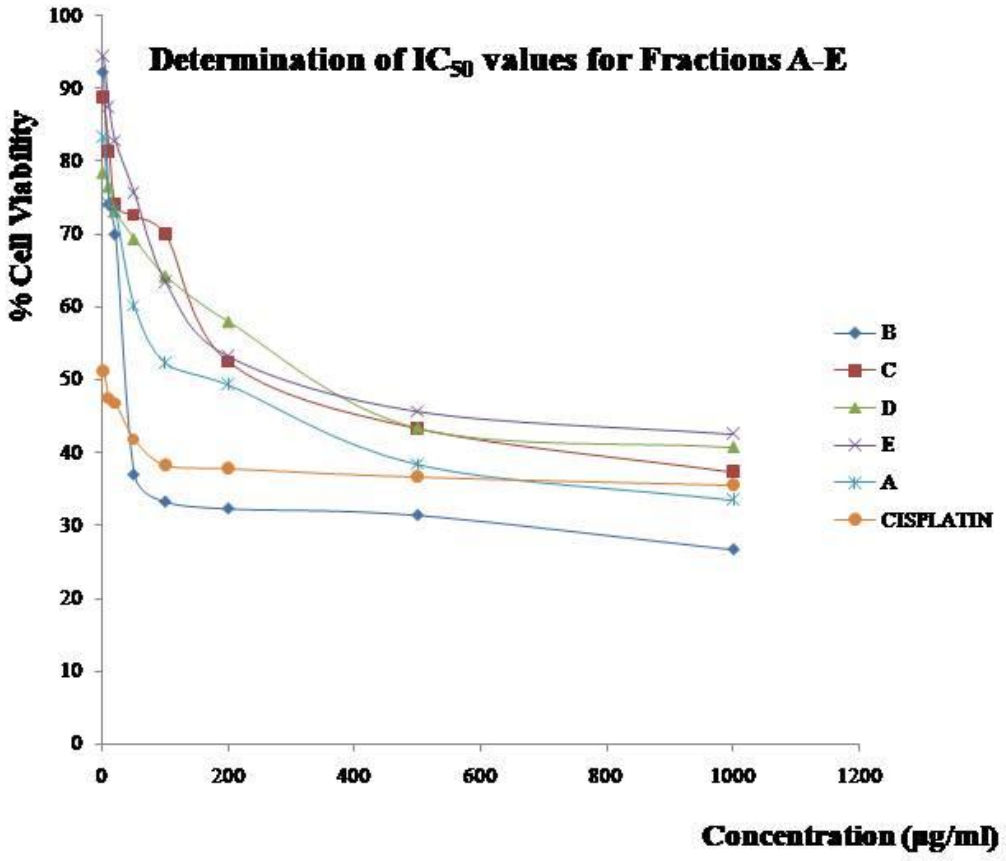

Figure 1 Plot of Percentage (%) Cell viability against different concentrations of Fractions A-E

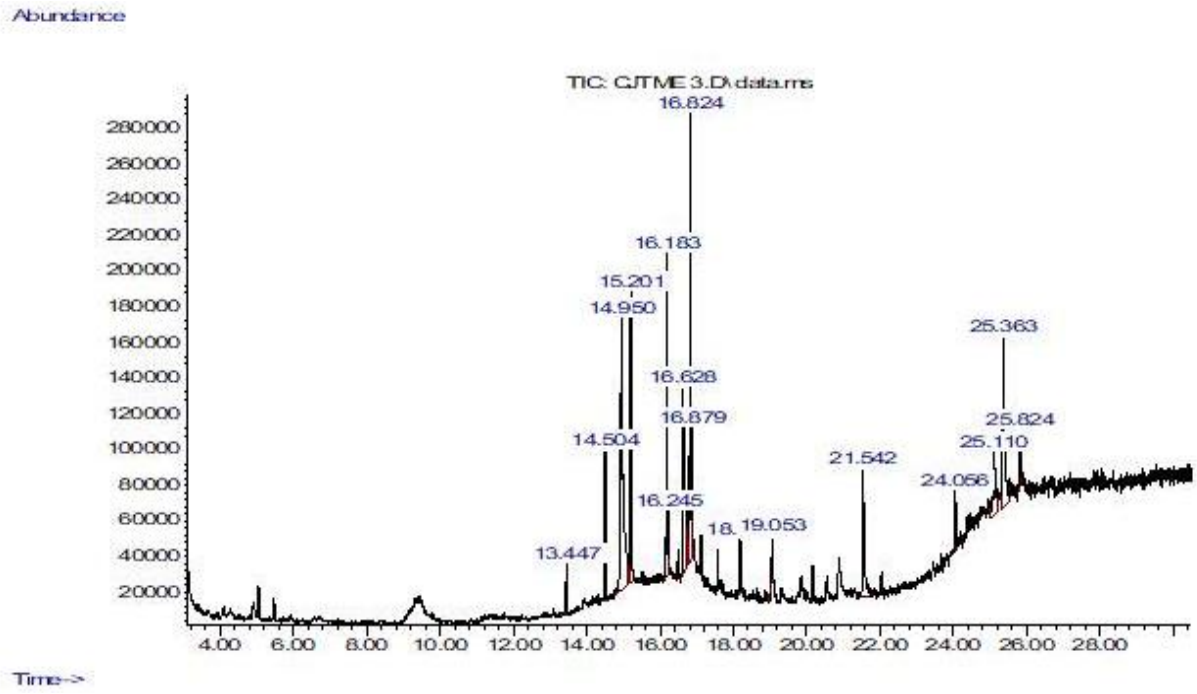

Figure 2 Total ion Chromatogram of Fraction B analyzed in GCMS

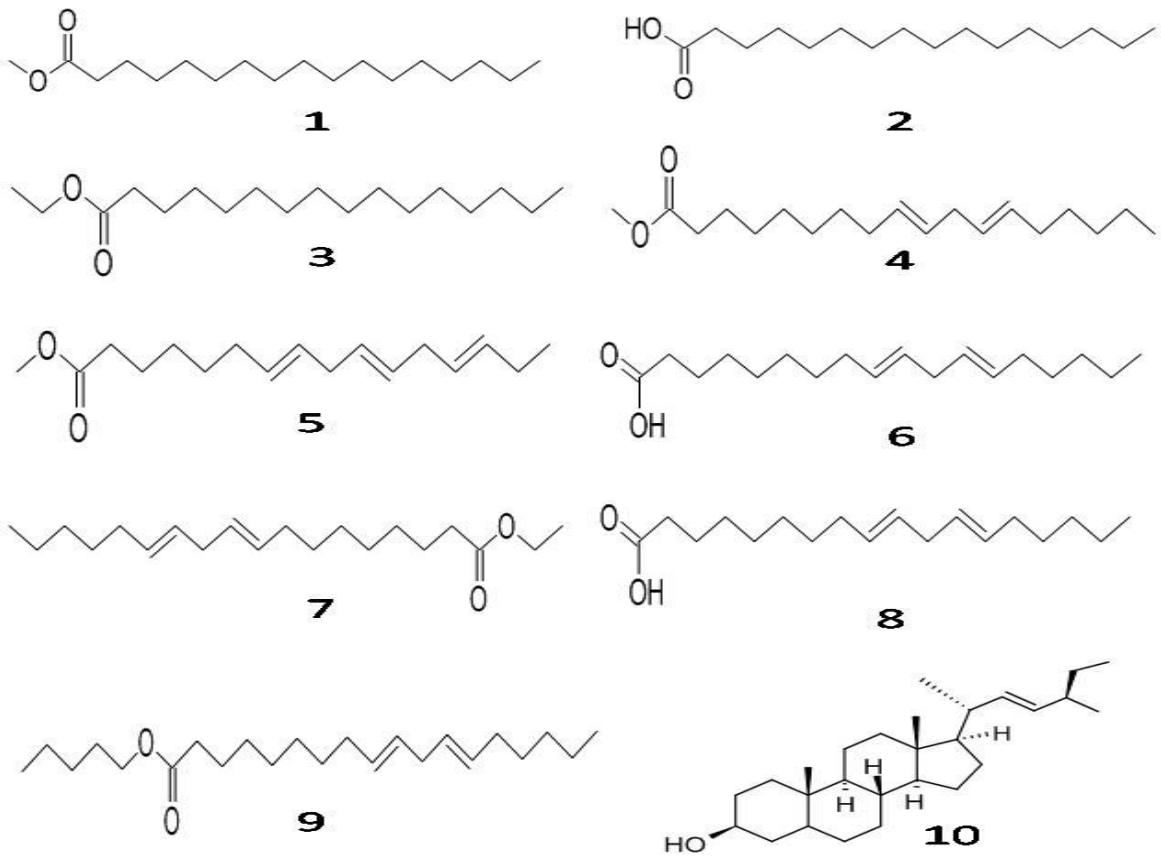

Figure 3 Compounds identified in Fraction B of *C. jagus* by GCMS analysis

Table 2 Compounds identified in Fraction B by GCMS analysis

tR(min.)	Peak area (%)	Name of Compound	NIST matching (%)
14.502	3.95	Hexadecanoic acid, methyl ester	98
14.948	18.96	n-Hexadecanoic acid	99
15.200	7.90	Hexadecanoic acid, ethyl ester	98
16.184	8.79	9,12-Octadecadienoic acid (Z,Z)-,methyl ester	99
16.247	1.61	7,10,13-Hexadecatrienoic acid, methyl ester	92
16.625	13.95	9,12-Octadecadienoic acid (Z,Z)-	98
16.825	13.94	Linoleic acid ethyl ester	99
16.877	3.48	Linoelaidic acid	92
19.051	0.45	Pentyllinoleate	94
25.362	9.41	Stigmasterol	90

Compounds Identified in Fraction B by LCMS Analysis

The total ion chromatograms for Fraction B, analyzed using LC-MS in both positive and negative ionization modes, are shown in (Figure 4). Only nine compounds from the LC-MS chromatogram of Fraction B (in both positive and negative modes) were putatively identified (Table 3). The structures of the compounds (1-9) are shown in (Figure 5). These include 3′,4′-Dimethoxy-7-Hydroxyflavone

(1), 5-methoxyflavanone (2), 2',5-dimethoxyflavone (3), 5,6-dimethoxy flavones (4), 4',7-Dimethoxy-5-hydroxyflavone (5), 3',7-Dimethoxy-3-hydroxyflavone (6), 5,6,7-trimethoxyflavone (7), 4',5,7-Trimethoxyflavone (8) andLiquiritigenin (9). The mass spectra of the compounds (1-9) identified in Fraction B by LCMS analysis are in (Appendix 1).

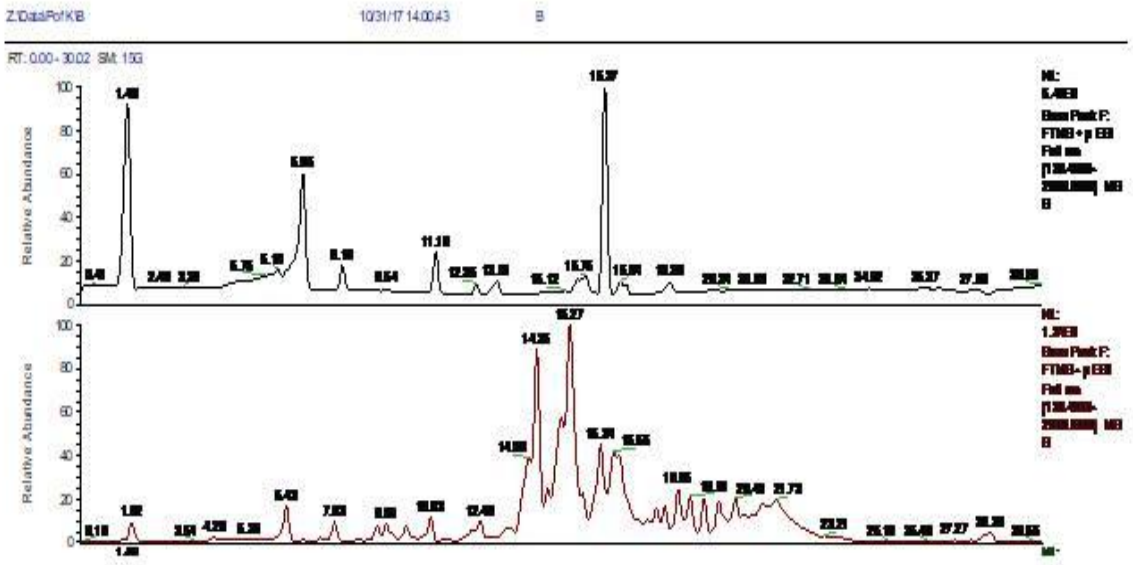

Figure 4 Total ion chromatogram of Fraction B obtained from LCMS analysis in the positive and negative ionization modes.

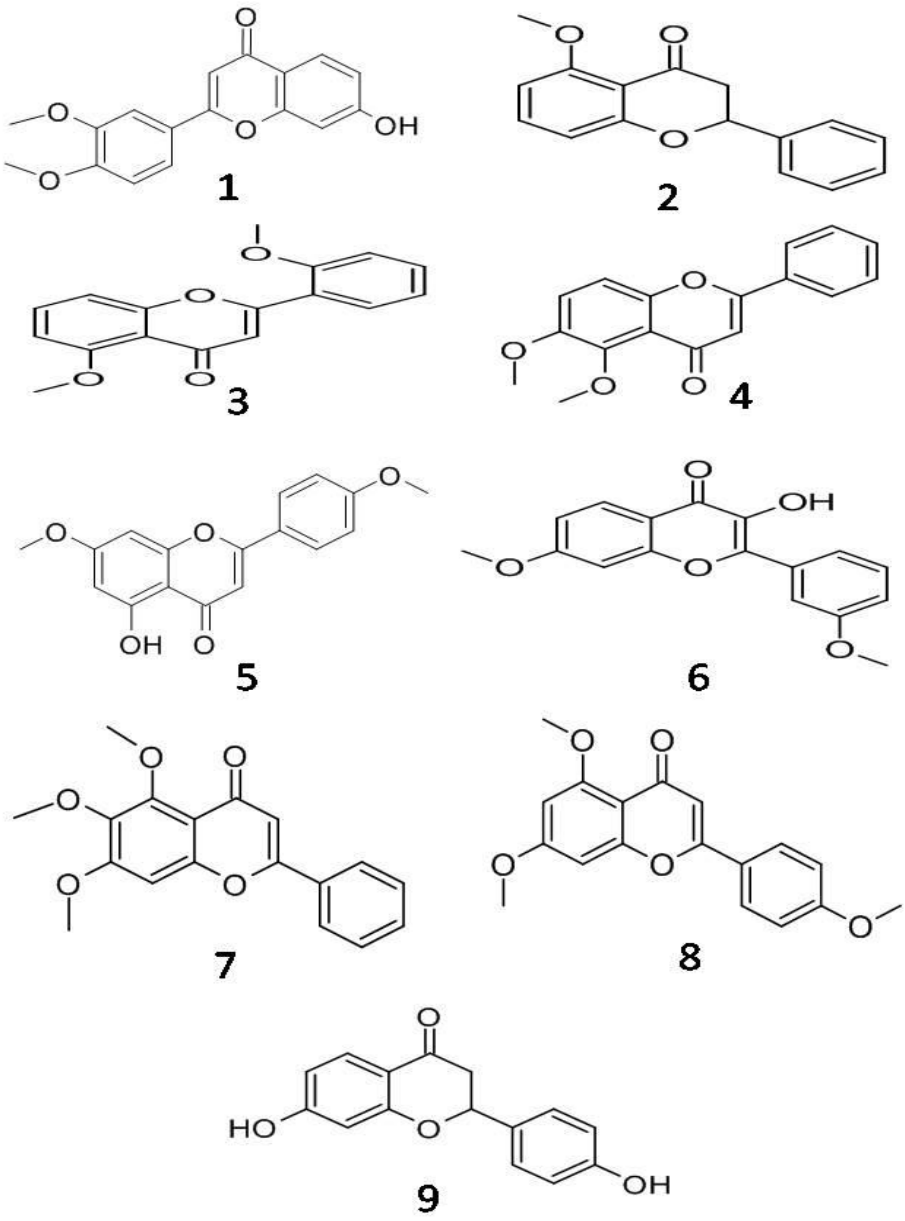

Figure 5 Compounds identified in Fraction B by LCMS

Table 3 Compounds putatively identified in Fraction B by LCMS analysis in the positive and negative ionization modes

No	Proposed Compound	Retention time (min)	Formula	Molecular Weight	Major Fragments
1	3′,4′-Dimethoxy-7-Hydroxyflavone	1.48	C17H14O5	298.29	299.11[M+H]+, 241.09 [M+H-CO-CH3-CH3]+
2	5-methoxyflavanone	9.53	C16H14O3	254.28	507.30 [2M+H] 253.14 [M-H] 209.15 [M-H-CO-CH3]-

3	2',5-dimethoxyflavone	11.10	C17H14O4	282.29	587.36 [2M+Na]+ 305.17 [M+Na]+ 241.07[M+H-CO-CH3]+
4	5,6-dimethoxy flavone	12.49	C17H14O4	282.29	281.14 [M-H]-
5	4',7-Dimethoxy-5-hydroxyflavone	14.00	C17H14O5	298.29	297.15 [M-H]- 265.15 [M-H-H2O-CH3]-
6	3',7-Dimethoxy-3-hydroxyflavone	14.25	C17H14O5	298.29	297.15 [M-H]- 265.15 [M-H-H2O-CH3]-
7	5,6,7-trimethoxyflavone	14.99	C18H16O5	312.3	311.17[M-H]-
8	4',5,7-Trimethoxyflavone	15.27	C18H16O5	312.3	311.17[M-H]-
9	Liquiritigenin	16.24	C15H12O4	256.25	511.47 [2M-H]- 325.18 255.23 [M-H]-

Molecular Docking of Identified Compounds with the Proteins

Table 4 displays the binding energy of the identified compounds with 1NMS, 2AR9 and 4LQM. From the table, it can be observed that hexadecanoic acid (-7.96 kcal/mol), 9,12-octadecadienoic acid (-7.78 kcal/mol), and linoelaidic acid (-8.23 kcal/mol) exhibited better binding energies than the standard drug, Sorafenib, which had binding energy of -7.72 kcal/mol against the Caspase-3 enzyme. Similarly, hexadecanoic acid methyl ester (-8.10 kcal mol-1), and pentyl linoleate (-8.00 kcal mol-1) had comparable binding energy with Sorafenib (-8.47 kcal mol-1) against the Caspase-9 enzyme (2AR9). In addition, hexadecanoic acid (-8.29 kcal mol-1), linoelaidic acid (-8.58 kcal mol-1), and pentyl linoleate (-8.66 kcal mol-1) had better binding energy with EGFR than Sorafenib (which had a binding energy of -8.24 kcal mol-1 with EGFR). The two-dimensional (2D) interaction diagram of the complexes formed by these compounds with the Caspase-3, Caspase-9 and EGFR enzymes are shown in Figures 6, 7, and 8, respectively.

***In silico* screening of Most active compounds for drug-likeness**

The compounds that demonstrated better activity than the standard drugs were screened for drug-likeness. The results of this evaluation are presented in (Table 5).

Extraction

The extraction of dried plant material was performed using solvents of increasing polarity at each stage, starting with hexane as a non-polar solvent, followed by ethyl acetate as a medium-polarity solvent, and concluding with methanol as a polar solvent. This step-wise extraction ensures the distribution of the phytoconstituents according to their polarity in the concentrated extracts. The results showed that the bulb of *Crinum jagus* is rich in polar constituents.

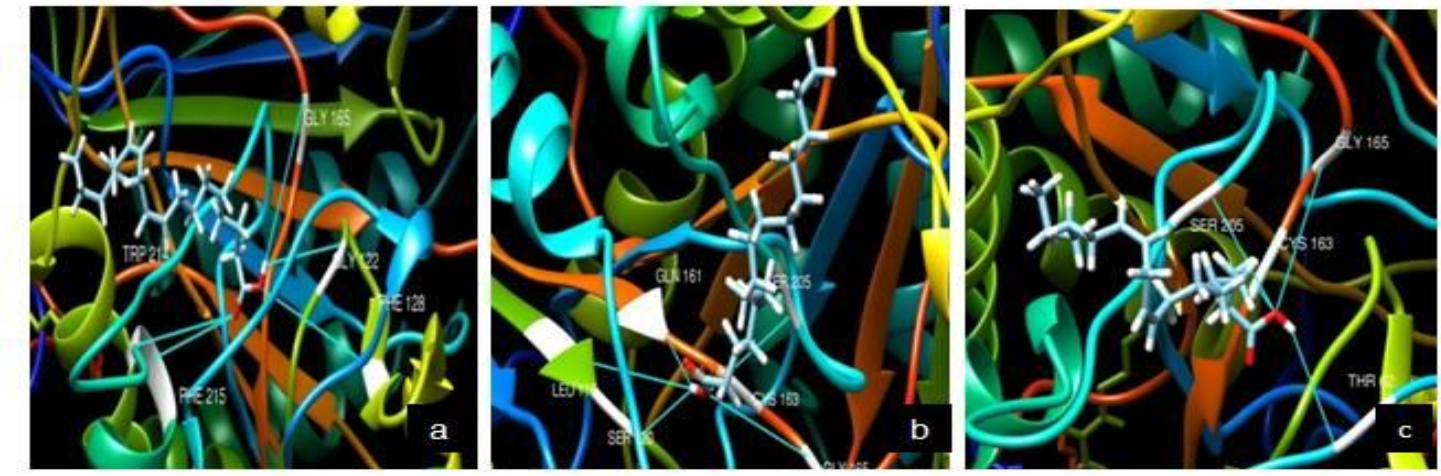

Figure 6 The two-dimensional (2D) interaction diagram of the complexes formed between Linoelaidic acid (A), hexadecanoic acid (B) and 9,12-Otadecanoic acid (C) and Caspase-3

Table 4 Binding Affinities of Identified compounds with 1NMS, 4LQM and 2AR9

Ligand	1NMS	2AR9	4LQM
Hexadecanoic acid methyl ester	-7.56	-8.10	-8.02
Hexadecanoic acid	-7.96	-7.56	-8.29
Hexadecanoic acid ethyl ester	-7.60	-7.86	-8.00
9,12-Octadecadienoic acid (Z,Z)-,methyl ester	-7.38	-7.62	-7.97
7,10,13-Hexadecatrienoic acid, methyl ester	-7.50	-7.44	-7.68
9,12-Octadecadienoic acid (Z,Z)-	-7.78	-7.78	-7.96
Linoleic acid ethyl ester	-7.52	-7.84	-8.20
Linoelaidic acid	-8.23	-7.63	-8.58
Pentyl linoleate	-7.59	-8.00	-8.66
3’,4’-Dimethoxy-7-Hydroxyflavone	-7.38	-7.24	-7.84
5-Methoxyflavanone	-6.52	-7.38	-6.71
2’,5-dimethoxyflavone	-6.32	-7.03	-7.73
5,6-dimethoxy flavone	-6.35	-7.13	-7.65
3',7-Dimethoxy-3-hydroxyflavone	-7.05	-7.08	-7.84
4’,5,7-trimethoxyflavone	-7.13	-7.62	-7.64
5,6,7-trimethoxyflavone	-6.86	-7.29	-8.00
4,7-dimethoxy-5-hydroxyflavone	-7.14	-7.14	-7.51
Liquiritigenin	-6.93	-7.45	-7.14
Sorafenib	-7.72	-8.47	-8.24

Table 5 Evaluation of Compounds for Drug-likeness

Ligand	M.W (<= 500)	HBD (<=5)	HBA (<=10)	NRB (<=10)	TPSA	iLogP (<=5)	MR (40-130)	Violations
Hexadecanoic acid methyl ester	270.45	0	2	15	26.30	4.41	85.12	Yes; 1 violation: MLOGP>4.15
Hexadecanoic acid	256.42	1	2	14	37.30	3.85	80.80	Yes; 1 violation: MLOGP>4.15
9,12-Octadecadienoic acid (Z,Z)-	280.45	1	2	14	37.30	4.14	89.46	Yes; 1 violation: MLOGP>4.15
Linoelaidic acid	280.45	1	2	14	37.30	4.14	89.46	Yes; 1 violation: MLOGP>4.15
Pentyl linoleate	350.58	0	2	19	26.30	5.71	113.01	Yes; 1 violation: MLOGP>4.15

Anticancer Studies of Fractions against HepG2 cell line

Following glass chromatographic separation of the methanol extract, five fractions (A-E) were obtained. The anti-proliferative properties of these fractions were estimated by screening them for activity against the HepG2 cell line. The IC50 value, which measures the concentration of each fraction that would kill 50% of the cell line, was used to grade the cytotoxic potentials of the fractions against the HepG2 cell line. This value was obtained by plotting the percentage of viable cells against various concentrations of the fractions. The IC50 value obtained for Fraction B is 37 μg/ml. According to the United States National Cancer Institute Guidelines, Fraction B with IC50< 100 μg/mL has anti-proliferative properties. Since the biological properties displayed by plants are due to their phytoconstituents, Fraction B is subjected to GCMS and LCMS analysis to identify the compounds responsible for their anticancer properties.

GCMS and LCMS Analysis of Fraction B

Only ten (10) out of the sixteen (16) peaks on the GCMS chromatogram could be identified. Most compounds identified in the fraction by GCMS are fatty acids and fatty acid esters. Fatty acids and fatty esters have been documented in bulbs of *Crinum* species. For example, eicosanoic acid ethyl ester, n-hexadecanoic acid, caryophyllene, 9,12-Octadecadienoic acid, and undecanoic acid ethyl ester have been identified in the volatile oil of the bulb of *C. ornatum*Ait. by GCMS (Oloyede et al., 2010). Nine (9) phenolic compounds, including flavonoids, were putatively identified in the positive and negative ion chromatograms from the LCMS analysis of Fraction B (Table 5). Compound 1 (Rt = 1.48 min) with molecular ion [M+H]+ at 299.11 had a fragment ion at 241.09 corresponding to the loss of CO and two methyl groups and was putatively identified as 3′,4′-Dimethoxy-7-hydroxyflavone.

For Compound 2 (Rt = 9.53 min), the molecular ion peak was 253.14 [M-H]-. The compound had a fragment ion at 209.15, corresponding to the loss of CO and CH3 groups. The peak at 507.30 is the [2M + H]+ peak. The Compound was putatively identified as 5-methoxyflavanone. The molecular ion [M+Na]+ peak for Compound 3 (Rt = 11.10 min) appeared at 305.17 (the [2M+Na]+ peak was at 587.36). The peak at 241.07 corresponds to the loss of CO and CH3. The structure of Compound 3 was putatively identified as 2',5-dimethoxyflavone. In Compound 4 (Rt = 12.49), the prominent peak at 281.14 was assigned as the [M-H]-, and the structure of the compound was putatively identified as 5,6-dimethoxyflavone. The molecular ion peak [M-H]- for Compound 5 (Rt = 14.00 min) is 297.15. A fragment peak corresponding to the loss of H2O and CH3 was found at 265.15. The structure of the compound was putatively identified as 4′,7-Dimethoxy-5-hydroxyflavone.

Compound 6 (Rt = 14.25 min) is possibly an isomer of compound 5 and was putatively identified as 3',7-Dimethoxy-3-hydroxyflavone. Compounds 7 and 8 had their molecular ion peaks [M-H]- at 311.17. The compounds were putatively identified as 5,6,7-trimethoxyflavone and 4',5,7-trimethoxyflavone, respectively. Compound 9, with a molecular ion [M-H]- peak at 255.23 and [2M-H]- peak at 511.47, was tentatively identified as Liquiritigenin. Liquiritigenin has been reported in the bulbs of related *Crinum* species (Refaat et al., 2012; Min et al., 2001). The compounds detected following GCMS and LCMS profiling of Fraction B are mainly fatty acids, fatty acid esters, and flavonoids. The anticancer properties of flavonoids and fatty acids are well documented in the literature (De-Luna et al., 2023).

***In silico* Investigation of Compounds Identified in Fraction B as Potential Anticancer Agents**

Though the exact molecular mechanism supporting the occurrence, progression, and metastasis of hepatocellular carcinoma is not entirely understood, several genes, factors, and pathways involved in its development have been identified (Ogunwobi et al., 2019). Cancer disrupts several physiological processes in the body, altering the apoptotic/non-apoptotic protein balance and suppressing caspase functions, evading apoptosis. Caspases are attractive targets for apoptosis-related diseases including neurodegenerative diseases, inflammation, and cancers. The epidermal growth factor receptor (EGFR) controls various essential cellular functions including proliferation, chemotactic migration, invasion and the avoidance of apoptosis (Burgess, 2008; Han and Lo, 2012). There is a correlation between elevated expression of EGFR and poor prognosis in several types of cancers.

Two-dimensional Interaction of Compounds with Caspase-3 Enzyme

From the two-dimensional (2D) interaction diagram of the complexes formed by linoelaidic acid, hexadecanoic acid, and 9,12-Octadecadienoic acid with the Caspase-3 enzyme (Figure 6), it is observable that carboxylic acid functional groups of the compounds are responsible for their hydrogen bond interaction with the amino acid residues of the Caspase-3 enzyme. More specifically, the carboxylic group of linoelaidic acid interacted with PHE215, TRP214, PHE128, GLY165, and GLY122; the carboxylic acid group of hexadecanoic acid interacted with SER205, GLY165, CYS163, SER120, LEU118, and GLN163, while the carboxylic acid functional group of 9,12-Octadecadienoic acid interacted with GLY165, CYS163, SER205, and THR62.

Two-dimensional Interaction of Compounds with the Caspase-9 Enzyme

Hexadecanoic acid methyl ester and pentyl linoleate formed hydrogen bonds with the amino acid residues of the Caspase-9 enzyme through their functional groups. Hexadecanoic acid methyl ester interacted with the ALA241 and CYS402 residues, while Pentyl linoleate formed a hydrogen bond with GLY350. The two-dimensional (2D) interaction diagram of the complexes formed by these compounds with the enzymes is shown in (Figure 7).

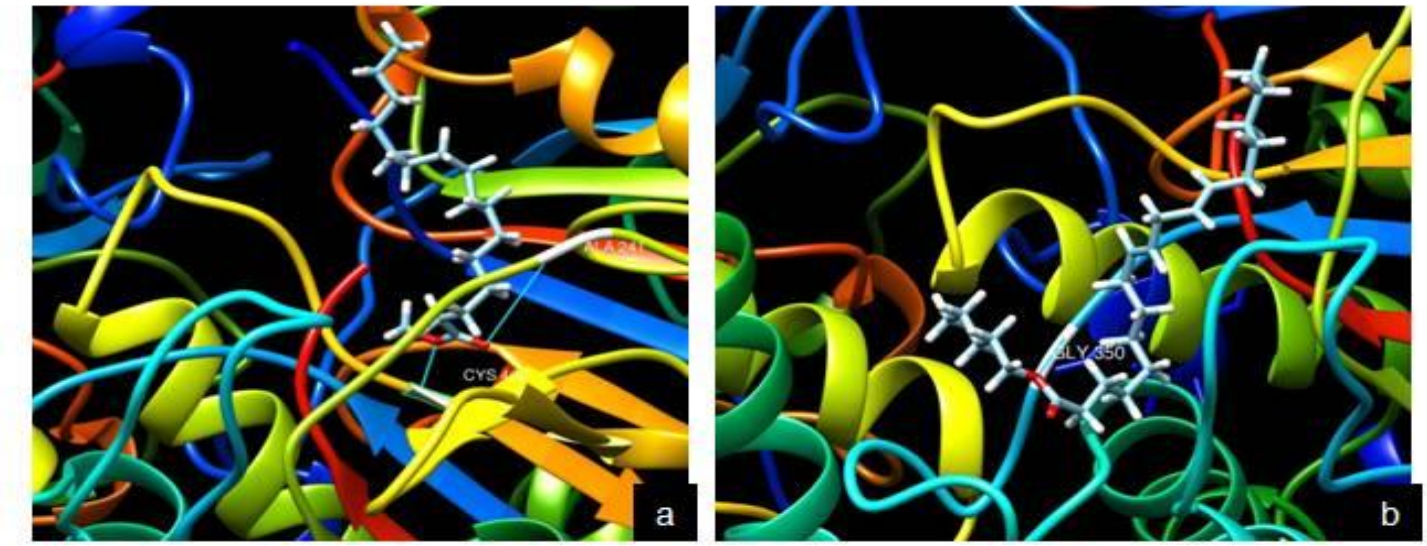

Figure 7 The two-dimensional (2D) interaction diagram of the complexes formed between hexadecanoic acid methyl ester (A) and pentyl linoleate (B) and Caspase-9 (2AR9)

Two-dimensional Interaction of Compounds with the EGFR

Pentyl linoleate formed hydrogen bonds with the amino acid residues, ASP800, VAL845, MET793, and GLU746 of the EGFR enzyme via its ester function group. The carboxylic acid functional group in hexadecanoic acid interacted (through hydrogen bonds) with the amino residues, VAL845 and CYS797 of the enzyme. Linoelaidic acid also formed hydrogen bonds with ASP837, LEU799, and ASP800

via its carboxylic acid functional group. The two-dimensional (2D) interaction diagrams of the complexes formed by these compounds with the enzymes are shown in (Figure 8).

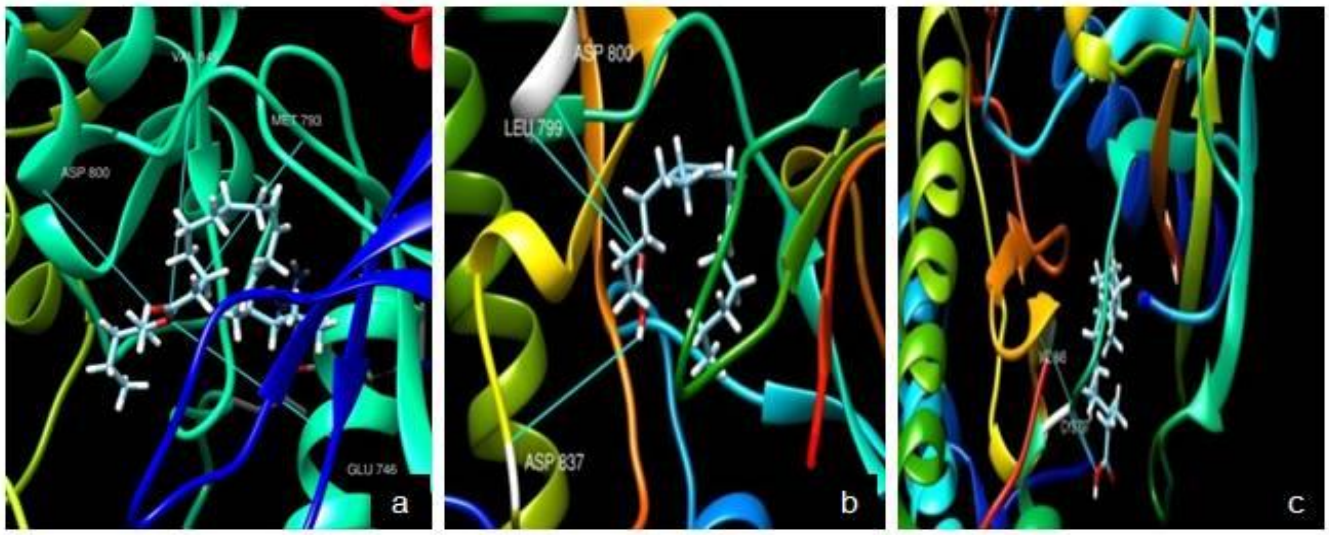

Figure 8 The two-dimensional (2D) interaction diagram of the complexes formed between pentyl linoleate (A), linoelaidic acid (B) and hexadecanoic acid (C) and EGFR (4LQM)

Drug Likeness of Compounds

The results show that the hexadecanoic acid, linoelaidic acid, hexadecanoic acid methyl ester, pentyl linoleate, and 9,12-Octadecadienoic acid violated only one of the five rules stipulated by Lipinski. A compound that violates only one of the five rules could be considered a potential drug candidate (Mustafa et al., 2022).

4. CONCLUSION

Phytochemical screening of the most active fraction (B) of the methanol extract of *Crinum jagus* bulb by GCMS and LCMS led to the identification of 19 compounds, mainly fatty acids, fatty acid esters, and flavonoids. These compounds may have contributed to the activity of Fraction B against HepG2 cells. *In silico* investigation on the compounds showed that linoelaidic acid, hexadecanoic acid, and 9,12-Octadecadienoic acid had better binding affinity for Caspase-3 than the standard drug, sorafenib. The study found that hexadecanoic acid methyl ester and pentyl linoleate exhibited similar binding energy with Sorafenib. In contrast, hexadecanoic acid, linoelaidic acid, and pentyl linoleate showed better binding energy with EGFR. These results support the traditional medicinal use of this plant for cancer treatment.

Acknowledgement

The authors thank Mr. Owolabi of the Botanical Gardens, University of Ibadan for assisting with sample collection.

Author contributions

Both authors participated in the design of the study. Taye Alawode carried out the experimental studies and wrote the first draft of the manuscript. Both authors read and approved the final manuscript.

Ethical approval & declaration

In this article, as per the plant regulations followed in Federal University Otuoke, Nigeria & Federal University of Technology Akure, Nigeria, the authors were collected the *Crinum jagus* (J. Thomp.) Dandy bulbs in November 2016 from the Botanical Gardens at the University of Ibadan, Nigeria. The plant samples were identified by Mr Kayode Owolabi, a taxonomist working with the Garden.

Samples (with voucher number UIH-22441) were subsequently deposited at the University Herbarium. The ethical guidelines for plants & plant materials are followed in the study for species collection & experimentation. The HepG2 cell line was obtained from the American Type Culture Collection (ATCC) (USA). The ethical guidelines for cell lines are followed in the study for experimentation.

Informed consent

Not applicable

Conflicts of interests

The authors declare that there are no conflicts of interests.

Funding

The study has not received any external funding.

Data and materials availability

All data associated with this study are present in the paper.

APPENDIX 1

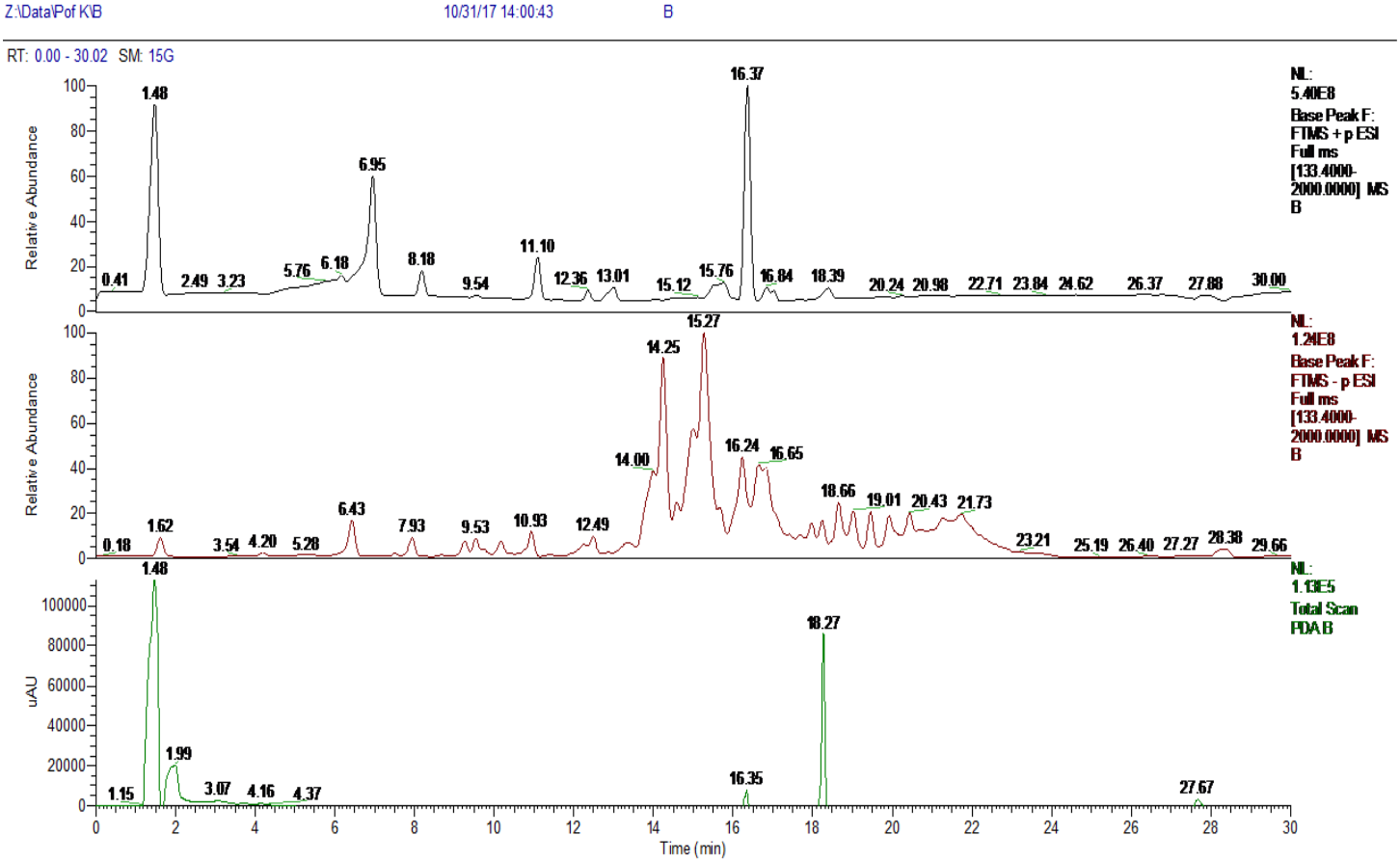

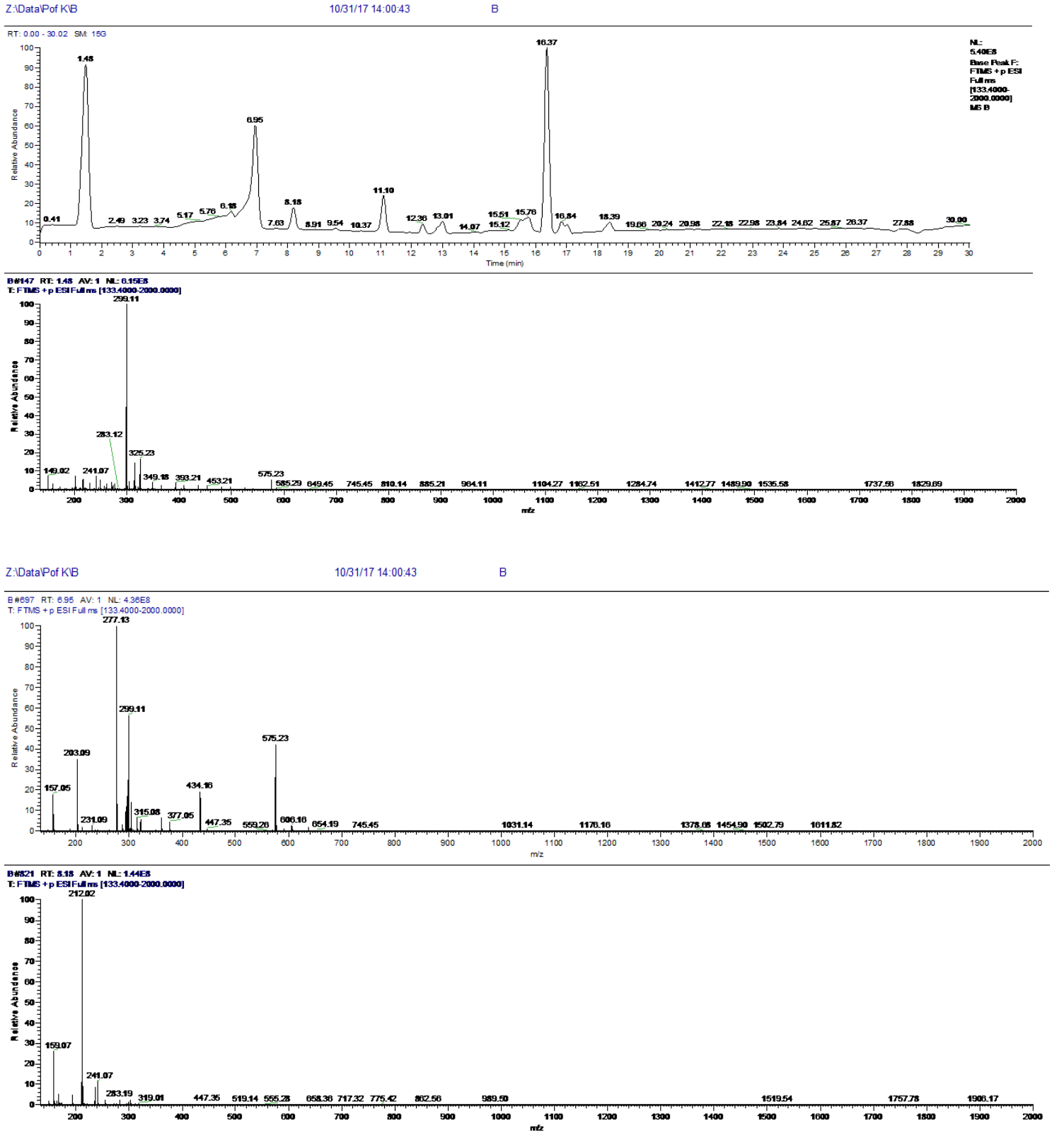
Z:\Data\Pof K\B
10/31/17 14:00:43
B
RT: 0.00 - 30.02 SM: 15G
Relative Abundance
Time (min)
NL: 5.40E8
Base Peak F: FTMS + p ESI Full ms [133.4000-2000.0000] MS B
B#147 RT: 1.48 AV: 1 NL: 6.15E8
T: FTMS + p ESI Full ms [133.4000-2000.0000]
299.11
283.12
325.23
149.02
241.07
575.23
m/z
Z:\Data\Pof K\B
10/31/17 14:00:43
B
B #697 RT: 6.95 AV: 1 NL: 4.36E8
T: FTMS + p ESI Full ms [133.4000-2000.0000]
277.13
299.11
203.09
575.23
157.05
434.16
231.09
315.08
377.05
447.35
559.26
606.16
654.19
745.45
1031.14
1176.16
1611.82
B#821 RT: 8.18 AV: 1 NL: 1.44E8
T: FTMS + p ESI Full ms [133.4000-2000.0000]
212.02
159.07
241.07
283.19
319.01
447.35
519.14
555.28
658.36
717.32
775.42
862.56
989.50
1519.54
1757.78
1986.17

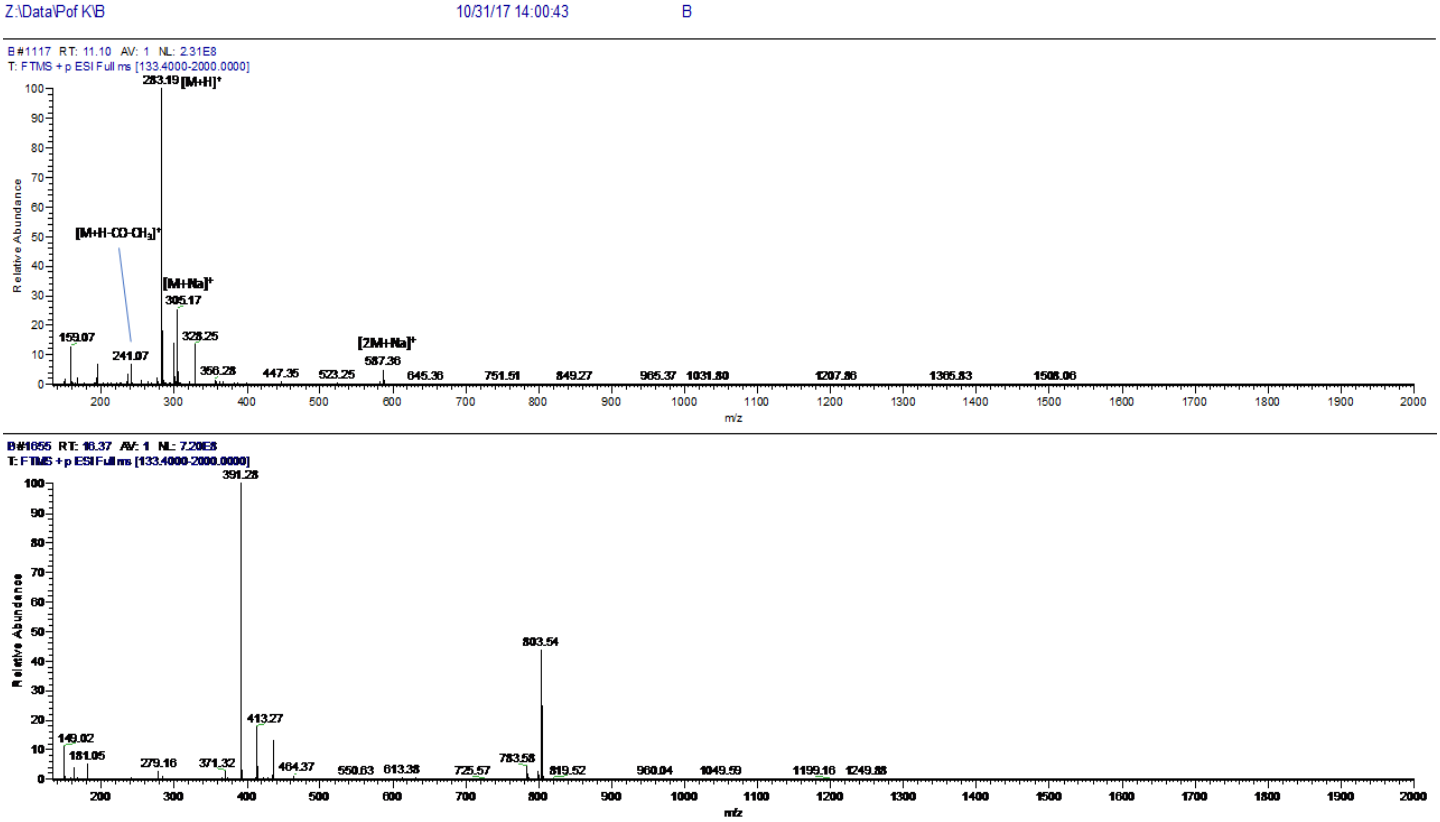
Z:\Data\Pof K\B
10/31/17 14:00:43
B
B#1117 RT: 11.10 AV: 1 NL: 2.31E8
T: FTMS + p ESI Full ms [133.4000-2000.0000]
283.19 [M+H]+
[M+H-CO-CH3]+
[M+Na]+
305.17
159.07
241.07
328.25
356.28
[2M+Na]+
587.36
Relative Abundance
m/z
B#1655 RT: 16.37 AV: 1 NL: 7.20E8
T: FTMS + p ESI Full ms [133.4000-2000.0000]
391.28
803.54
413.27
149.02
181.05
279.16
371.32
464.37
550.63
613.38
725.57
783.58
819.52
960.04
1049.59
1199.16
1249.88
Relative Abundance
m/z

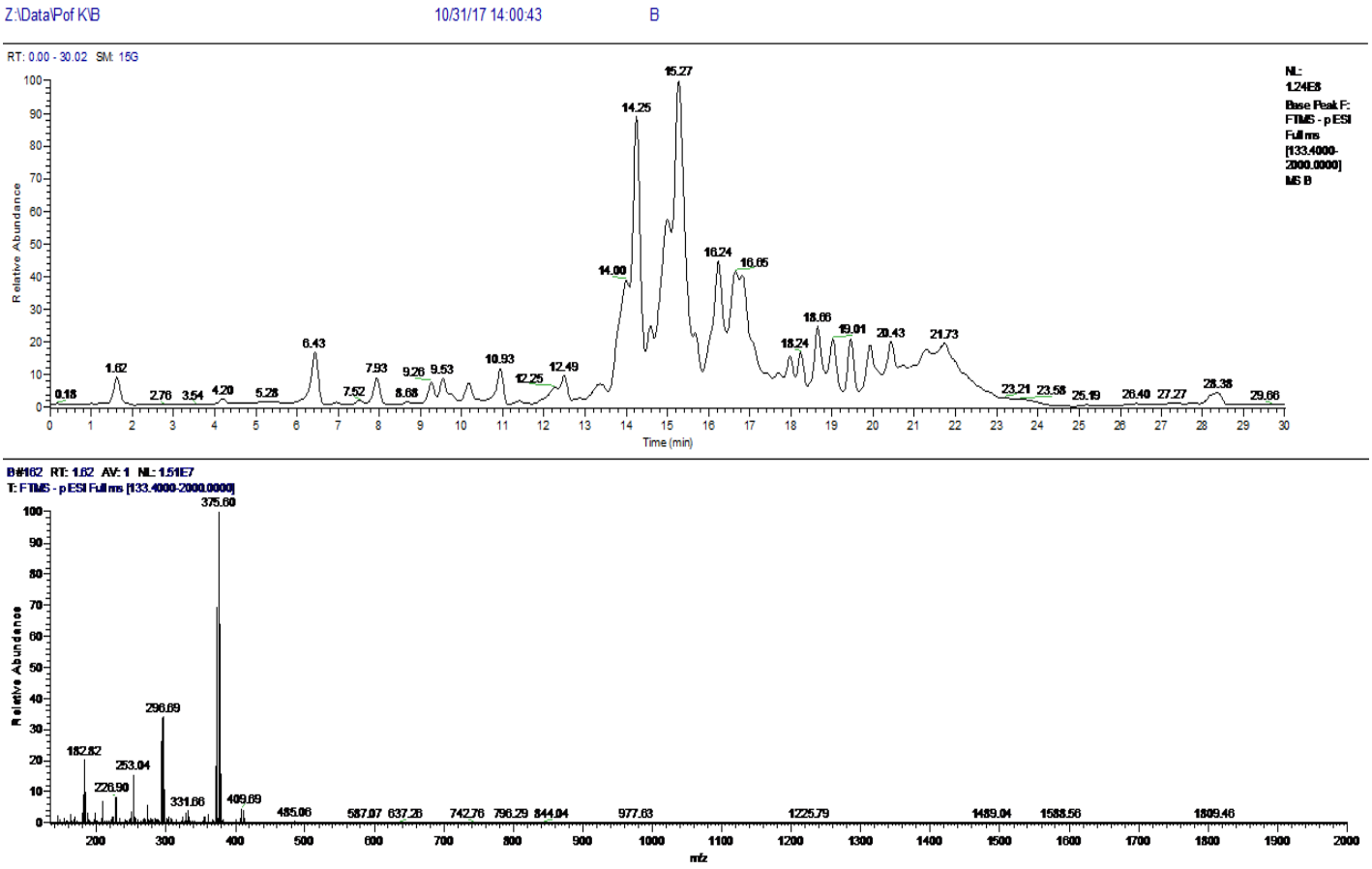
Z:\Data\Pof K\B
10/31/17 14:00:43
B
RT: 0.00 - 30.02 SM: 15G
NL:
1.24E8
Base Peak F:
FTMS - p ESI
Full ms
[133.4000-
2000.0000]
MS B
Relative Abundance
Time (min)
B#162 RT: 1.62 AV: 1 NL: 1.51E7
T: FTMS - p ESI Full ms [133.4000-2000.0000]
Relative Abundance
m/z

Z:\Data\Pof K\B 10/31/17 14:00:43 B

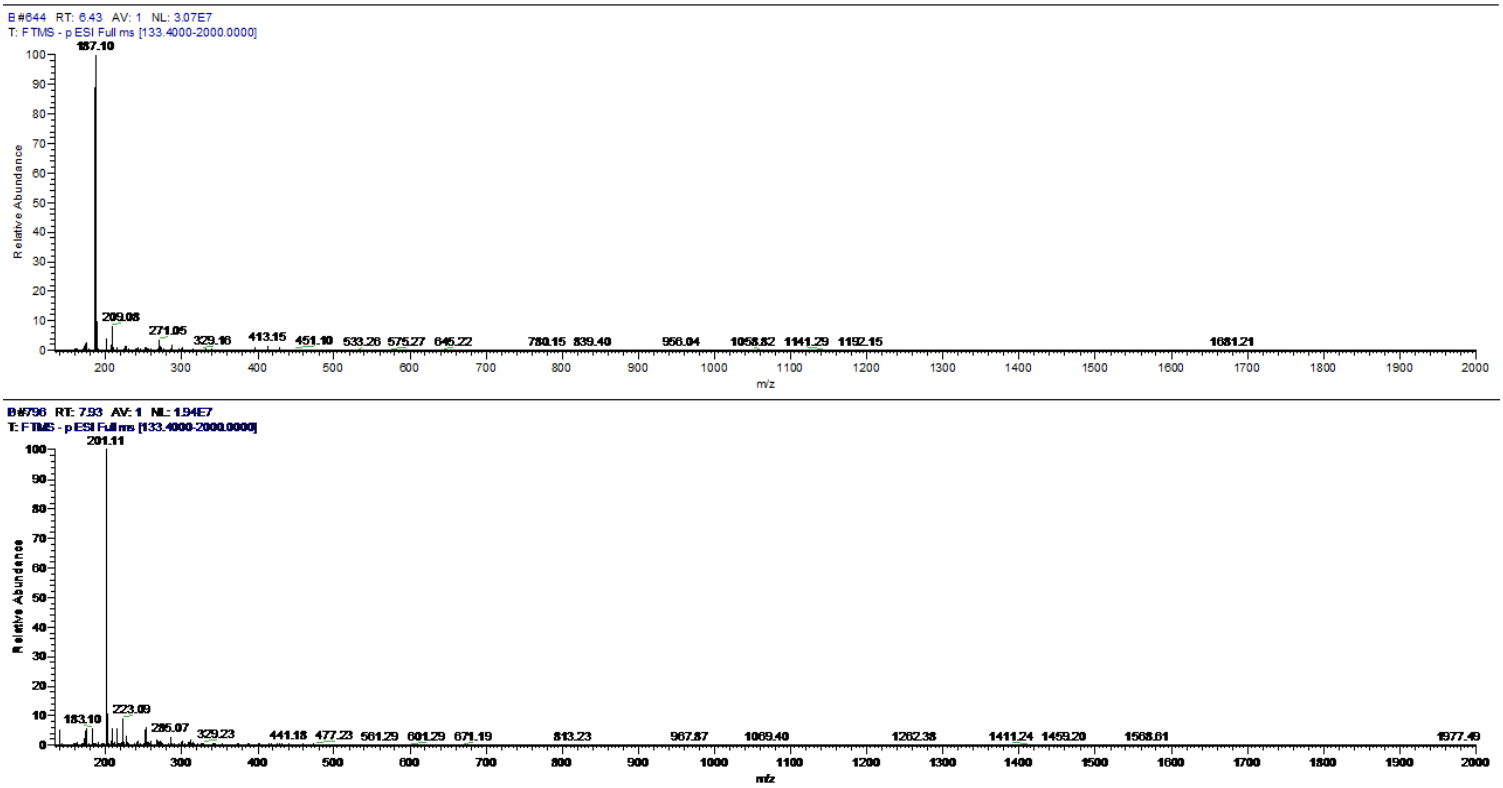

Z:\Data\Pof K\B 10/31/17 14:00:43 B

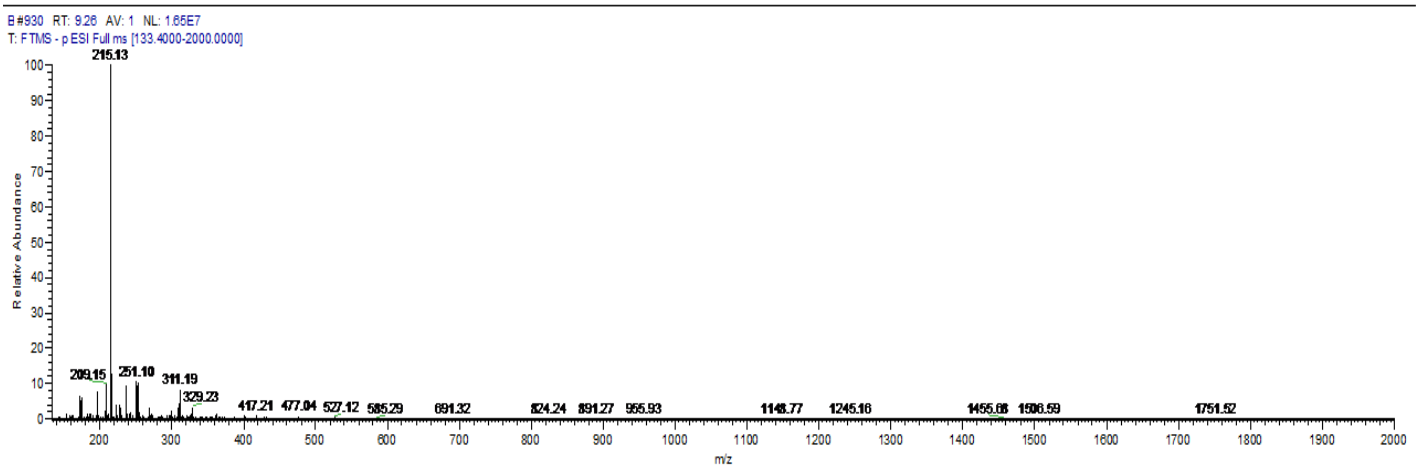

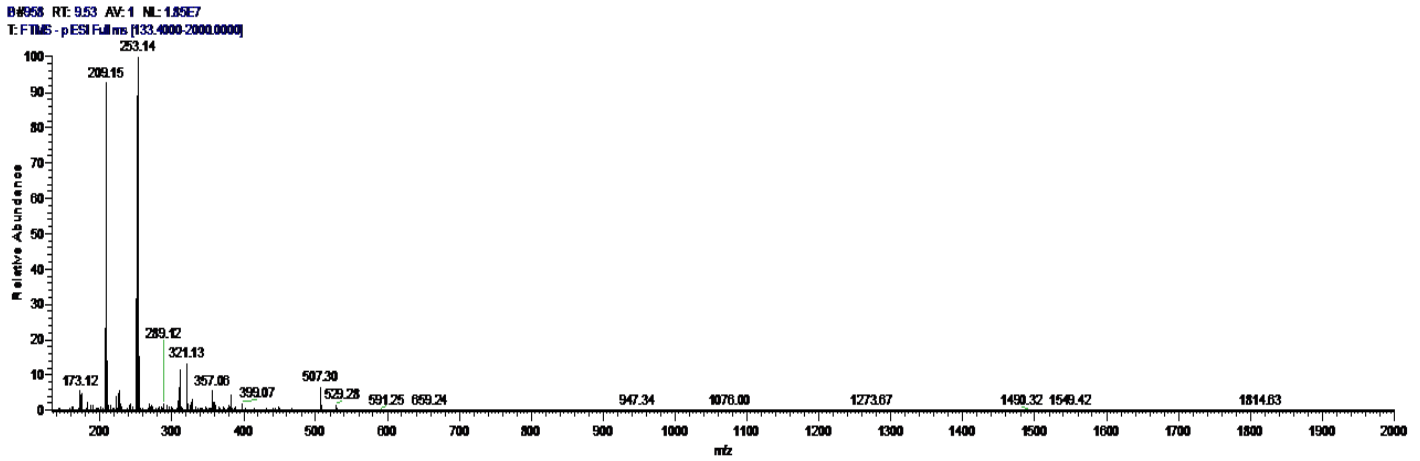

Z:\Data\Pof K\B 10/31/17 14:00:43 B

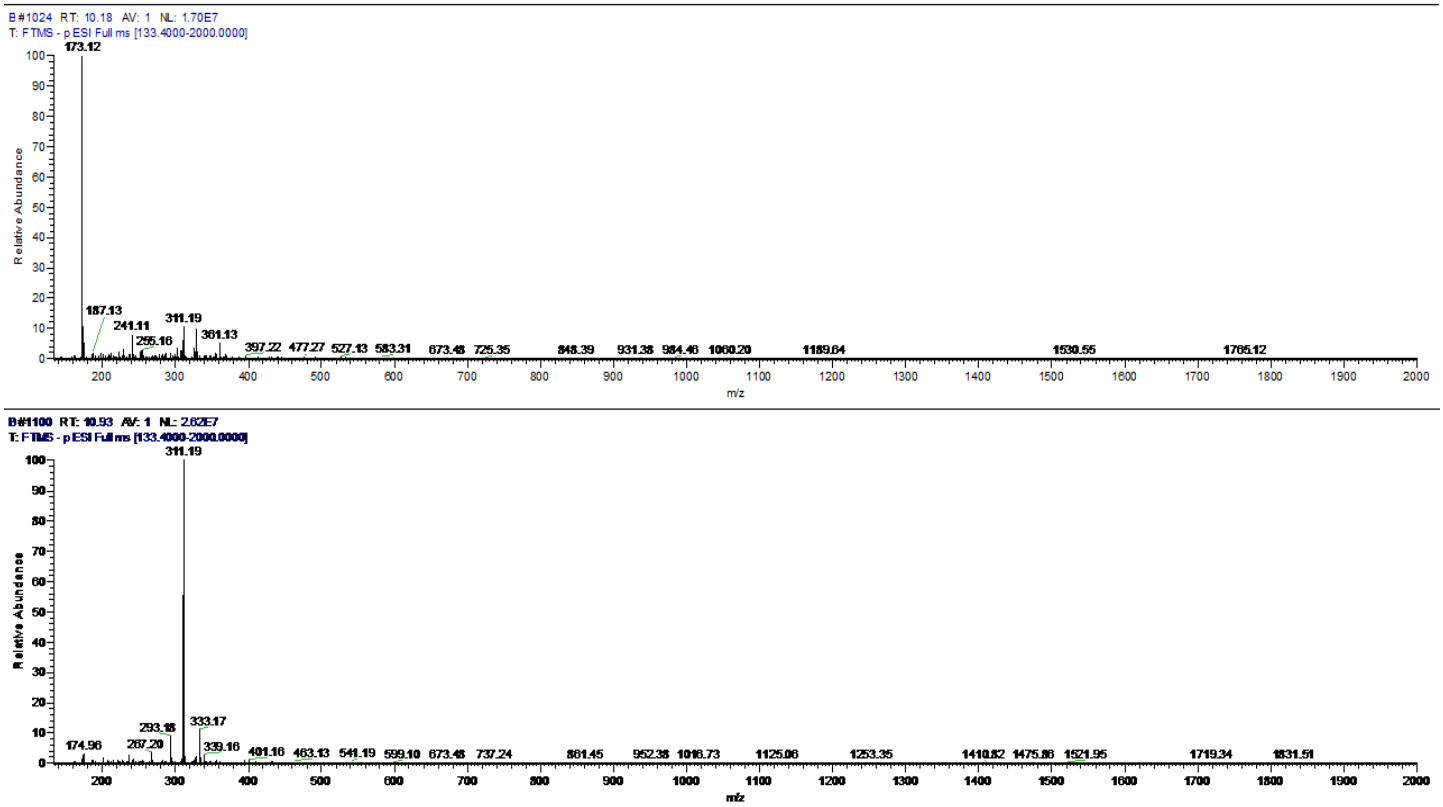

Z:\Data\Pof K\B 10/31/17 14:00:43 B

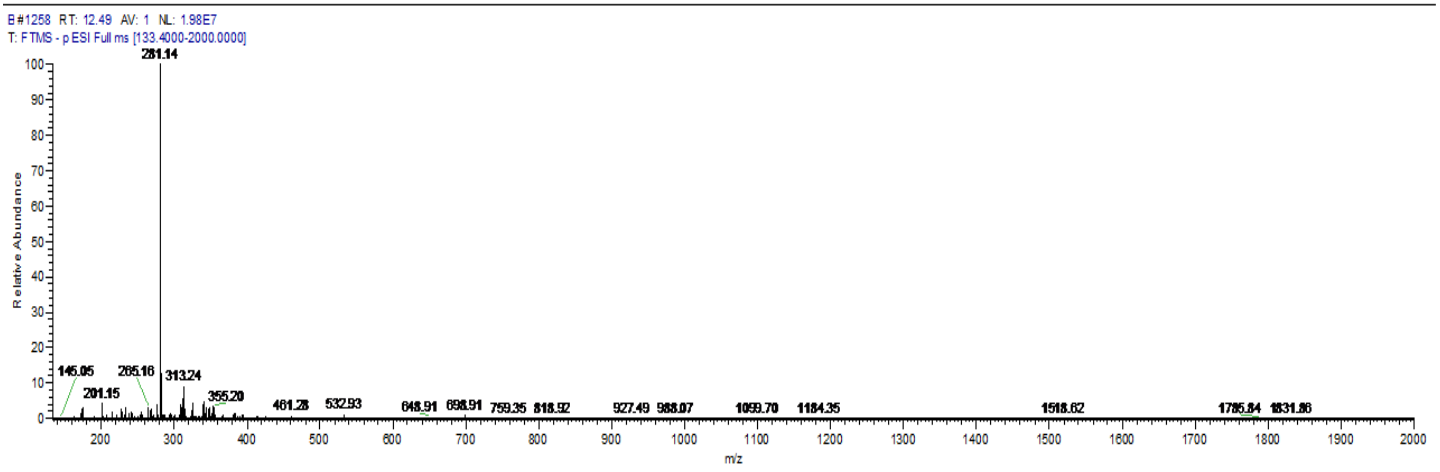

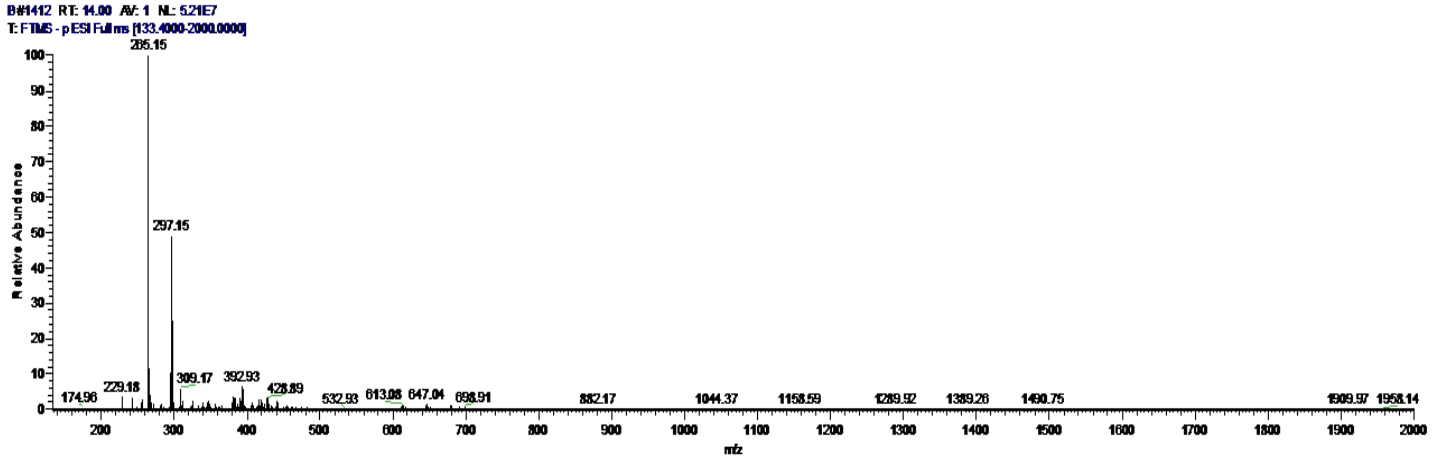

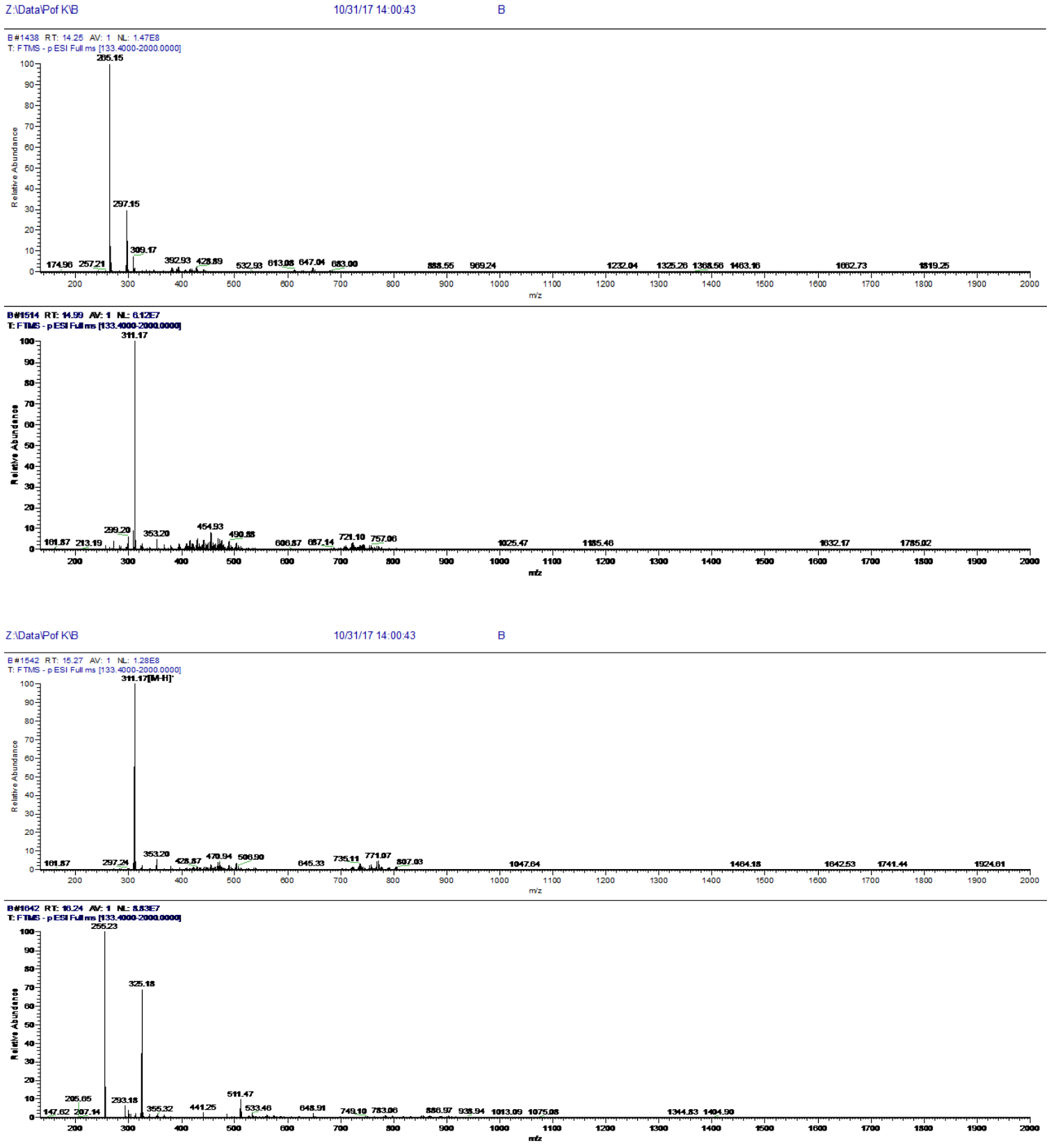
Z:\Data\Pof K\B 10/31/17 14:00:43 B
B #1438 RT: 14.25 AV: 1 NL: 1.47E8
T: FTMS - p ESI Full ms [133.4000-2000.0000]
285.15
297.15
309.17
Relative Abundance
m/z
B #1514 RT: 14.99 AV: 1 NL: 6.12E7
T: FTMS - p ESI Full ms [133.4000-2000.0000]
311.17
299.20
353.20
454.93
721.10
757.06
Relative Abundance
m/z
Z:\Data\Pof K\B 10/31/17 14:00:43 B
B #1542 RT: 15.27 AV: 1 NL: 1.28E8
T: FTMS - p ESI Full ms [133.4000-2000.0000]
311.17[M-H]-
353.20
470.94
506.90
735.11
771.07
Relative Abundance
m/z
B #1642 RT: 16.24 AV: 1 NL: 8.83E7
T: FTMS - p ESI Full ms [133.4000-2000.0000]
255.23
325.18
511.47
Relative Abundance
m/z

Z:\Data\Pof K\B 10/31/17 14:00:43 B

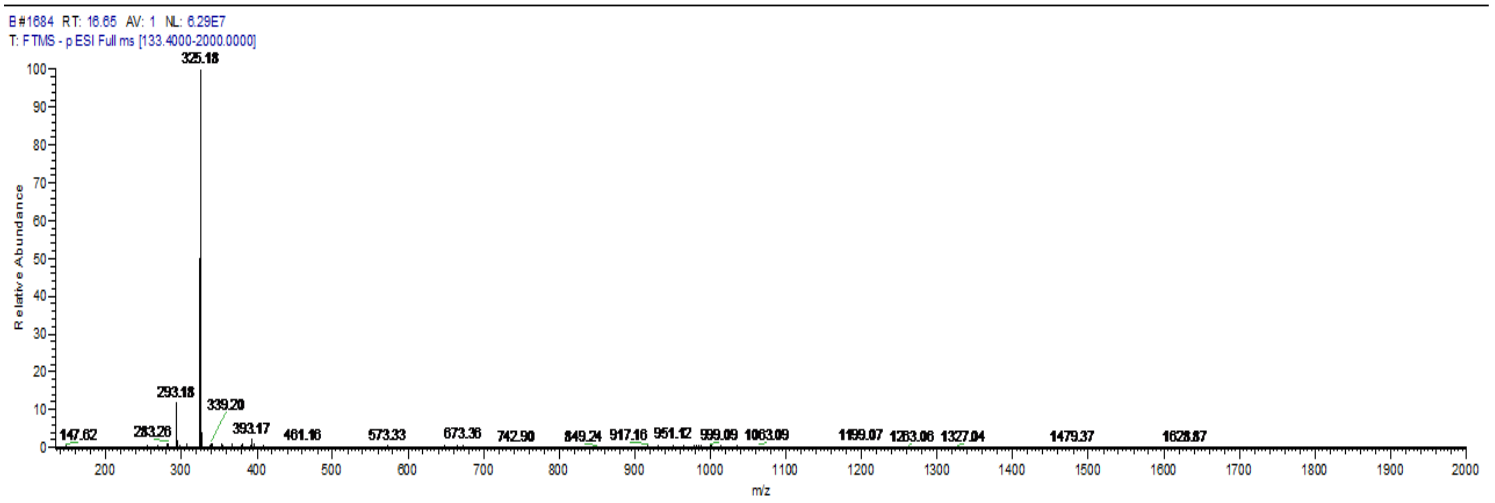

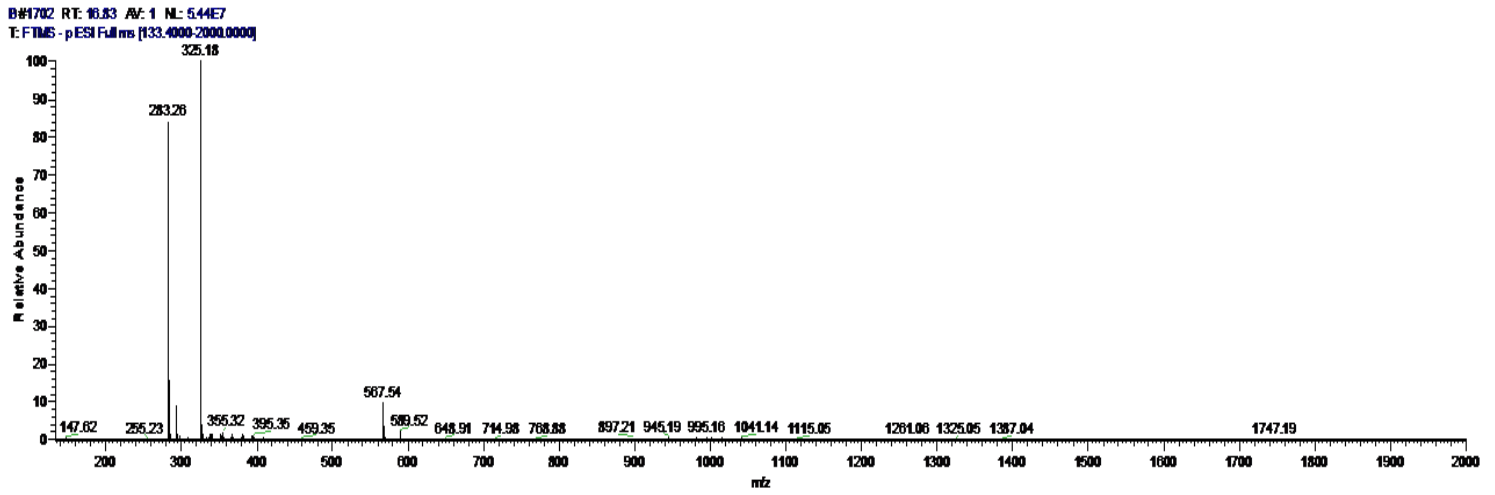

Z:\Data\Pof K\B 10/31/17 14:00:43 B

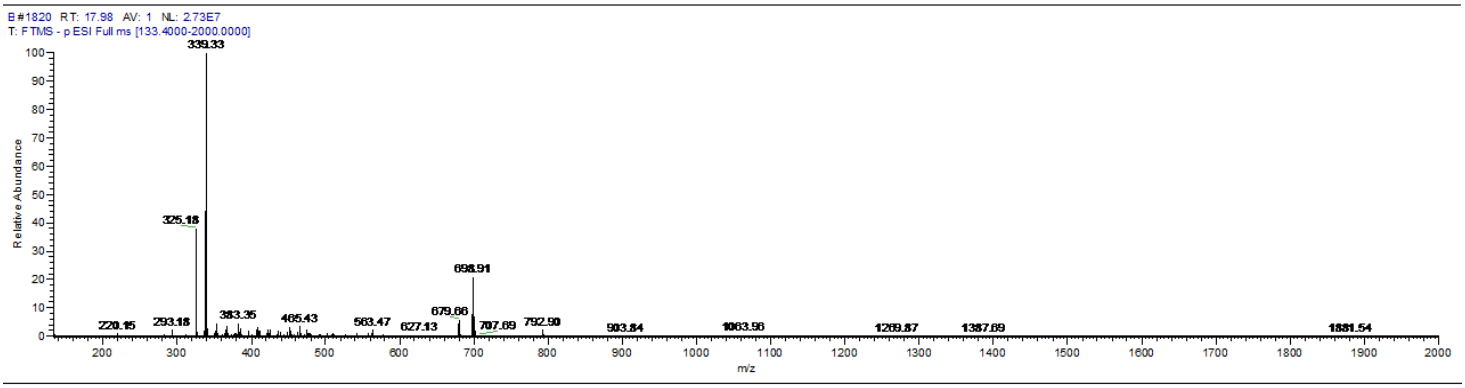

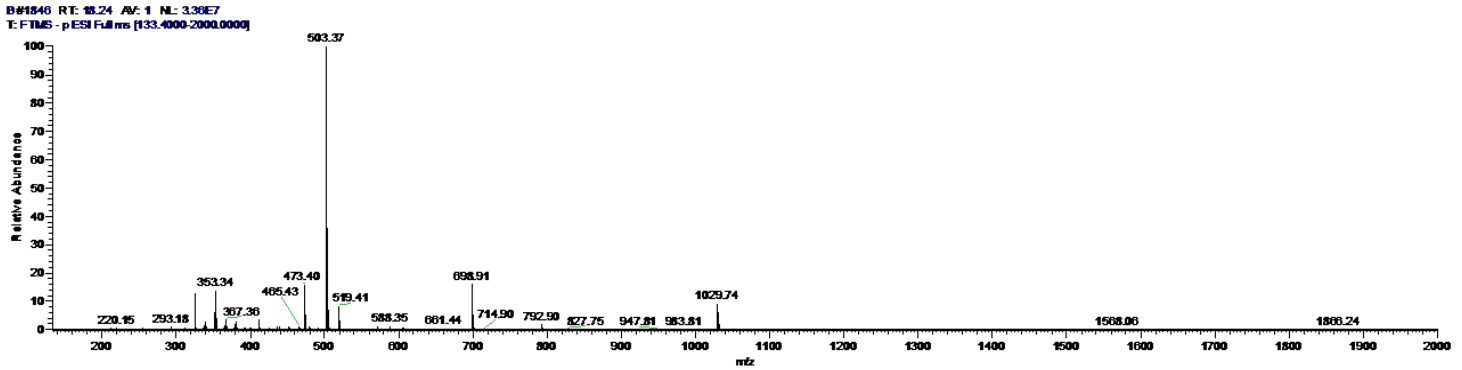

Z:\Data\Pof K\B 10/31/17 14:00:43 B

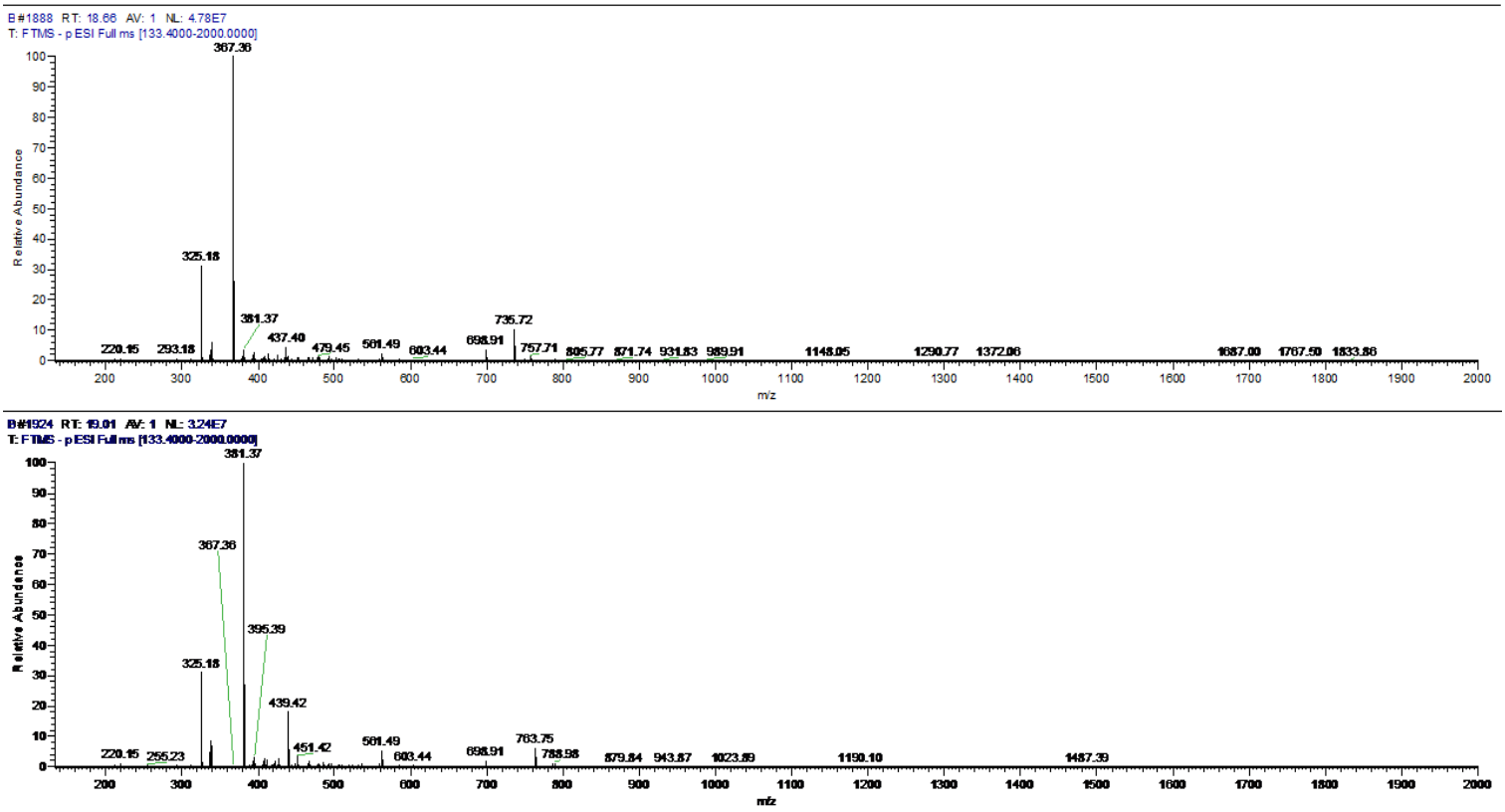

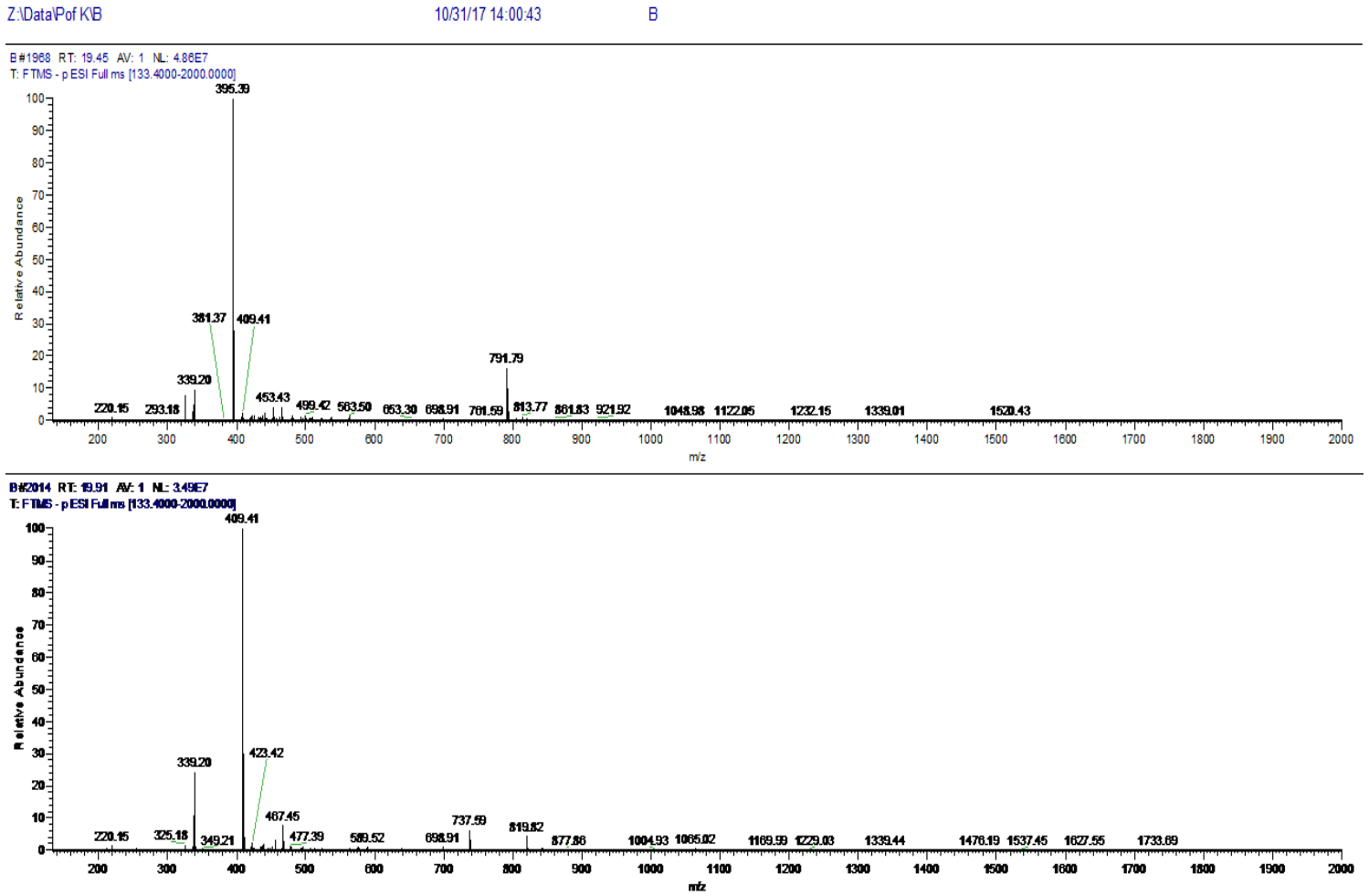

REFERENCES

1. Ahmad M. Cytotoxic activity of the leaf extract of *Crinum asiaticum* Linn. Aust J Med Herb 1996; 8(1):3-6.
2. Akintola AO, Kehinde AO, Adebiyi OE, Ademowo OG. Anti-tuberculosis activities of the crude methanolic extract and purified fractions of the bulb of Crinum jagus. Niger J Physiol Sci 2013; 28(2):135-140.
3. Alawode TT, Lajide L, Olaleye M, Owolabi B. Crinum jagus: antiproliferative studies of extracts on HepG2 cell line and in silico assessment of phytoconstituents as potential inhibitors of p53–mortalin interaction. Future J Pharm Sci 2023; 9:39. doi: 10.1186/s43094-023-00490-4
4. Burgess AW. EGFR family: structure, physiology, signalling and therapeutic targets. Growth Factors 2008; 26(5):263-74.
5. Daina A, Michielin O, Zoete V. SwissADME: a free web tool to evaluate pharmacokinetics, drug-likeness and medicinal chemistry friendliness of small molecules. Sci Rep 2017; 7(1):4 2717. doi: 10.1038/srep42717
6. De-Luna FCF, Ferreira WAS, Casseb SMM, De-Oliveira EHC. Anticancer Potential of Flavonoids: An Overview with an Emphasis on Tangeretin. Pharmaceuticals (Basel) 2023; 16(9):1 229. doi: 10.3390/ph16091229
7. Ghosal S, Kumar Y, Singh SK, Kumar A. Chemical constituents of Amaryllidaceae. Part 21. Ungeremine and criasbetaine, two anti-tumor alkaloids from Crinum asiaticum. J Chem Res (S) 1986; 3:112-211.
8. Grosdidier A, Zoete V, Michielin O. SwissDock, a protein-small molecule docking web service based on EADock DSS. Nucleic Acids Res 2011; 39:270-7.
9. Han W, Lo HW. Landscape of EGFR signaling network in human cancers: biology and therapeutic response in relation

to receptor sub-cellular locations. Cancer Lett 2012; 318:124-34. doi: 10.1016/j.canlet.2012.01.011

10. Howes MJR, Quave CL, Collemare J, Tatsis EC, Twilley D, Lulekal E, Andrew Farlow, Li L, Cazar M, Leaman DJ, Prescott TAK, Milliken W, Martin C, De-Canha MN, Lall N, Qin H, Walker BK, Vásquez-Londoño C, Allkin B, Rivers M, Simmonds MSJ, Bell E, Battison A, Felix J, Forest F, Leon C, Williams C, Lughadha EN. Molecules from nature: reconciling biodiversity conservation and global healthcare imperatives for sustainable use of medicinal plants and fungi. Plants People Planet 2020; 2(5):463-81.
11. Ka S, Masi M, Merindol N, Di-Lecce R, Plourde MB, Seck M, Górecki M, Pescitelli G, Desgagne-Penix I, Evidente A. Gigantelline, gigantellinine and gigancrinine, cherylline- and crinine-type alkaloids isolated from Crinum jagus with anti-acetylcholinesterase activity. Phytochemistry 2020; 175:112390. doi: 10.1016/j.phytochem.2020.112390
12. Kouadio ATG, Kabran GRM, Mamyrbekova-Bekro JA, Virieux D, Pirat JL, Bekro YA. Total alkaloids and in vitro antioxidant activity of Crinum jagus L. (Amaryllidaceae) organs from Côte d'Ivoire. Int J Green Herb Chem 2020; 9 (4):451-463.
13. Kumar BR. Application of HPLC and ESI-MS techniques in the analysis of phenolic acids and flavonoids from green leafy vegetables (GLVs). J Pharm Anal 2017; 7(6):349-364. doi: 10.10 16/j.jpha.2017.06.005
14. Mak D, Kramvis A. Epidemiology and aetiology of hepatocellular carcinoma in Sub-Saharan Africa. Hepatoma Res 2021; 7:39.
15. Min BS, Gao JJ, Nakamura N, Kim YH, Hattori M. Cytotoxic alkaloids and a flavan from the bulbs of Crinum asiaticum var. japonicum. Chem Pharm Bull (Tokyo) 2001; 49(9):1217-9. doi: 10.1248/cpb.49.1217
16. Mohammed ZK, Daja A, Hamza HG, Gidado A, Hussaini IM. Ethnomedicinal survey of folkloric plants used in managing breast cancers by the traditional medical practitioners of North-East Nigeria. J Med Appl Biosci 2014; 6(1):29-43.
17. Mustafa G, Mahrosh HS, Zafar M, Attique SA, Arif R. Exploring the antihyperglycemic potential of tetrapeptides devised from AdMc1 via different receptor proteins inhibition using in silico approaches. Int J Immunopathol Pharmacol 2022; 36:1-15. doi: 10.1177/03946320221103120
18. Mustafa G, Younas S, Mahrosh H, Albeshr M. Molecular Docking and Simulation-Binding Analysis of Plant Phytochemicals with the Hepatocellular Carcinoma Targets Epidermal Growth Factor Receptor and Caspase-9. Molecules 2023; 28:3583. doi: 10.3390/molecules28083583
19. Nair JJ, Campbell WE, Gammon DW, Albrecht CF, Viladomat F, Codina C, Bastida J. Alkaloids from Crinum delagoense. Phytochemistry 1998; 49(8):2539-2543.
20. Nawaz A, Jamal A, Arif A, Parveen Z. In vitro cytotoxic potential of Solanum nigrum against human cancer cell lines. Saudi J Biol Sci 2021; 28(8):4786-4792. doi: 10.1016/j.sjbs.2021.0 5.004
21. O'Boyle NM, Banck M, James CA, Morley C, Vandermeersch T, Hutchison GR. Open Babel: an open chemical toolbox. J Cheminform 2011; 3:33. doi: 10.1186/1758-2946-3-33
22. Ogunwobi OO, Harricharran T, Huaman J, Galuza A, Odumuwagun O, Tan Y, Ma GX, Nguyen MT. Mechanisms of hepatocellular carcinoma progression. World J Gastroenterol 2019; 25(19):2279-2293. doi: 10.3748/wjg.v25.i19.2279
23. Oloyede KG, Oladosu IA, Shodia AF. Chemical composition and cytotoxicity of the essential oils of Crinum ornatum (Ait.) Bury. Afr J Pure Appl Chem 2010; 4(3):35-37.
24. Osakwe O. The Significance of Discovery Screening and Structure Optimization Studies. In: Osakwe O, Rizvi SAA, editors. Social Aspects of Drug Discovery, Development and Commercialization. Academic Press 2016; 109-128. doi: 10.101 6/B978-0-12-802220-7.00005-3
25. Parikh ND, Tayob N, Singal AG. Blood-based biomarkers for hepatocellular carcinoma screening: Approaching the end of the ultrasound era? J Hepatol 2023; 78:207-216.
26. Patel KN, Patel JK, Patel MP, Rajput GC, Patel HA. Introduction to hyphenated techniques and their applications in pharmacy. Pharm Methods 2010; 1(1):2-13. doi: 10.4103/222 9-4708.72222
27. Refaat J, Kamel MS, Ramadan MA, Ali AA. Crinum; An Endless Source of Bioactive Principles: A Review. Part IV: Non-Alkaloidal Constituents. Int J Pharm Sci Res 2012; 4(3):94 1-948.
28. Sadybekov AV, Katritch V. Computational approaches streamlining drug discovery. Nature 2023; 616(7958):673-685. doi: 10.1038/s41586-023-05905-z
29. Salawu KM, Atunwa SA, Eniayewu IO. Cytotoxicity and antiproliferative studies of Crinum jagus L (Amaryllidaceae) bulb extract. Bima J Sci Technol 2020; 4(1):131-40.